NASA CR 111977-1

SUMMARY FINAL REPORT

BIOWASTE RESISTOJET PROPELLANT SYSTEM

BIOLOGICAL AND FUNCTIONAL ANALYSIS

TASK III

July 1972

Prepared Under Contract NAS1-10431

by

THE BIONETICS CORPORATION

18 Research Drive

Hampton, Virginia 23366

for

NATIONAL AERONAUTICS AND SPACE ADMINISTRATION

LANGLEY RESEARCH CENTER

Hampton, Virginia

23365

PREFACE

This summary final report, Biowaste Resistojet Propellant System Biological and Functional Analysis, is submitted by The Bionetics Corporation to the National Aeronautics and Space Administration, Langley Research Center, Hampton, Virginia, as required by Contract Number NAS1-10431. The work was conducted under the technical direction of Mr. Earl VanLandingham of the Space Technology Division of Langley Research Center. This final report is a summary of the work accomplished during Task III of the study and reported in detail in the interim monthly progress reports required under the contract.

Requests for further information concerning this report or the details contained in interim reports may be directed to

J. R. Wrobel

Resistojet Systems Project Engineer

CONTENTS

		PAGE
1.0	Background	1
	1.1 Study Guidelines	3
	1.2 Study Scope and Objectives	4
	1.3 Task Descriptions	5
	1.3.1 Literature Review and Problem Survey	6
	1.3.2 Analysis and Modeling	6
	1.3.3 Exhaust Contamination Limits on Biowaste Resistojet Operating Parameters	6
	1.3.4 Experiments Definition and Criteria	7
	1.4 Schedule of Task Performance	7
2.0	Technical Summary	9
	2.1 Literature Review and Problem Survey	9
	2.2 Analysis and Modeling	16
	2.2.1 Propellant Gas Property Analysis	16
	2.2.2 Modeling Viscous Expansion Processes	20
	2.2.3 Free Expansion	24
	2.2.4 Entrained Particulate Trajectories	27
	2.2.5 Vapor Condensation in the Exhaust	34
	2.2.6 Condensation on Adjacent Components	36
	2.2.7 Exhaust Lifetime in the Vicinity	37
	2.3 Model Applications	40
	2.3.1 Biowaste Resistojet Plume Flows	40
	2.3.2 Condensation of the Exhaust	42
	2.3.3 Particle Trajectories Computation	45

CONTENTS (CONT'D.)

		PAGE
3.0	Testing and Flight Experiments	50
	3.1 Ground Test Recommendations	51
	3.2 Flight Test Experiment	52
4.0	Conclusions and Recommendations	53
	4.1 Condensation Effects	53
	4.2 Particle Trajectories	54
	4.3 Effluent Life In The Vicinity	54
5.0	Bibliography	56

FIGURES

		PAGE
FIGURE 1	STUDY PERFORMANCE AND MILESTONE SCHEDULE	8
FIGURE 2	PRIOR HISTORY OF SPACECRAFT CONTAMINATION EFFECTS	10
FIGURE 3	PROPULSION EXHAUST CONTAMINATION STUDIES	15
FIGURE 4	REYNOLDS NUMBER FUNCTION $G(RE\#_D)$	21
FIGURE 5	POLYTROPIC EXPONENT VS. C_D	23
FIGURE 6	NOZZLE AREA RATIO FOR POLYTROPIC EXPANSION OF BIOWASTE GASES	25
FIGURE 7	CONSTANT DENSITY CONTOURS $\gamma = 1.20$	28
FIGURE 8	CONSTANT DENSITY CONTOURS $\gamma = 1.25$	29
FIGURE 9	CONSTANT DENSITY CONTOURS $\gamma = 1.3$	30
FIGURE 10	COMPARATIVE CONSTANT DENSITY CONTOURS	31
FIGURE 11	EFFECT OF VISCOSITY ON CONSTANT DENSITY CONTOURS	32

TABLES

		PAGE
TABLE 1	SPECIFIC HEAT RATIO FOR CANDIDATE BIOWASTE RESISTOJET PROPELLANT MIXTURES	18
TABLE 2	PROPELLANT DESCRIPTIONS	19
TABLE 3	VELOCITY RATIO	41
TABLE 4	PARTICULATE TURNING ANGLE FOR TYPICAL BIOWASTE MIXTURES AND PARTICLE SIZES	48

UNITS OF MEASUREMENTS

Units, abbreviations, and prefixes used in this report correspond to the International System of Units (SI) as prescribed by the Eleventh General Conference on Weights and Measures and presented in NASA Report SP-7012. The basic units for length, mass, and time are meter, kilogram and second respectively. Throughout the report, the English equivalent (foot, pound, and second) are presented for convenience.

The SI units, abbreviations, and prefixes most frequently used in this report are summarized below:

Basic Units

Length	meter	m
Mass	kilogram	kg
Time	second	s
Electric current	ampere	A
Temperature	degree Kelvin	^{o}K

Supplementary Units

Plane angle	radian	rad

Derived Units

Area	square meter	m^2
Volume	cubic meter	m^3
Frequency	hertz	Hz (s^{-1})
Density	kilogram per cubic meter	kg/m^3
Velocity	meter per second	m/s
Angular velocity	radian per second	rad/s
Acceleration	meter per second squared	m/s^2
Angular acceleration	radian per second squared	rad/s^2
Force	newton	N ($kg-m/s^2$)
Pressure	newton per sq meter	n/m^2
Kinematic Viscosity	sq meter per second	m^2/s
Dynamic Viscosity	newton-second per sq meter	$N-s/m^2$
Work, energy, quantity of heat	joule	J (N-m)
Power	watt	W (J/s)
Electric charge	coulomb	C (A-s)
Voltage, potential difference: electromotive force	volt	V (W/A)

Electric field strength	volt per meter	V/m	
Electric resistance	ohm		(V/A)
Electric capacitance	farad	F	(A-s/V)
Magnetic flux	weber	WB	(V-s)
Inductance	henry	H	(V-s/A)
Magnetic flux density	tesla	T	(Wb/m^2)
Magnetic field strength	ampere per meter	A/m	
Magnetomotive force	ampere	A	

Prefixes

Factor by which unit is multiplied	Prefix	Symbol
10^6	mega	M
10^3	kilo	k
10^{-2}	centi	c
10^{-3}	milli	m
10^{-6}	micro	

1.0 BACKGROUND

The use of a resistojet propulsion system for low thrust attitude control functions on long-term manned spaceflights in earth orbit has been identified and studied under several recent NASA contracts. Resistojets have been shown to effectively provide the low acceleration thrusting which is advantageous for applications where less than 10^{-5} 'g' is required for experimental purpose. The propulsive functions of such a resistojet system application could include atmospheric drag make-up and desaturation of rotary momentum storage (Control Moment Gyro) stabilization mechanizations.

An additional advantage of resistojets in manned flight applications is that gases and fluids residual to the crew environment control and life support mechanization can be used as the propellant media. These fluids, generically referred to as "biowastes", are available from a variety of spacecraft sources depending upon the crew support system mechanizations selected. The biowaste material must either be regenerated, vented into space or returned to earth via the logistics support system. On-board regeneration of biowaste generally requires the addition of process equipment and the consumption of electrical power. Venting into space can result in spacecraft external contamination, depending upon the fluid composition. Return-to-earth requires accumulation in the spacecraft, transfer to the logistic vehicle and transport to earth. The disposal solution for a particular biowaste material depends upon the consideration of the relative complexity of the above alternatives.

The diversion of biowastes through the resistojet propulsion system permits effective mass utilization, i.e., eliminates the separate disposal problem and removes the requirement to supply a separate propellant. Spacecraft contamination by the material vented through the resistojet system can be minimized by careful selection of biowaste sources and operation at temperatures above critical limits specific to the biowaste chosen.

The use of biowaste propellant in the resistojet propulsion system may introduce contamination problems internal to the propulsion system. A principal potential problem is the accommodation of the thruster heater elements and supply plumbing to contaminant laden throughputs. This contamination may detrimentally effect life and reliability through mechanical blockage of flow paths, by deposits, or by chemical attack and deterioration of the materials of construction.

Therefore, the specific selection of a biowaste material for resistojet propellant must meet several criteria:

a) the biowaste must constitute a significant mass, power, or cost factor to regenerate, or return to earth, thus being surplus to the spacecraft.

b) the resistojet biowaste effluent must not contribute to spacecraft external contamination, i.e., coatings, clouds, particulates, etc.

c) the biowaste must be chemically compatible with reasonably attainable plumbing and thruster fabrication technology.

In addition to these constraints, the biowastes selected must be available in sufficient quantity and duration in the mission to reliably provide the anticipated demands for impulse generating propellant.

Several studies and technology developments have been conducted, or are in progress, which bear on portions of the biowaste selection problems. NASA contracts NASL-10127 and NAS1-10170 have studied the biowaste resistojet conceptual design and mission interfaces, i.e. EC/LS interactions and modes, impulse demands, mass availability, etc. Other contracts have developed thruster materials and design technology. Two areas were not under detail study. One of these was the survey of the trace contaminants present in the

candidate biowastes and their potential impact upon the resistojet thruster, collection system and operating mode selection. The other was the analysis of the potential for spacecraft contamination by the resistojet exhaust.

To accomplish the survey and evaluation of the potential influence of biowaste contaminants on the propulsion system design and the evaluation of potential spacecraft contamination by resistojet exhaust, The Bionetics Corporation was awarded a study contract (NAS1-10431) by the National Aeronautics and Space Administration (NASA). Tasks I and II of the subject contract, comprising approximately 3/4 professional man-year of effort, studied the propulsion system internal effects of contaminant laden biowaste as it influenced component design, mechanization and life. The results of these studies are documented in NASA Contractor Report CR 111977 dated September 1971. Task III of the contract commenced in October 1971 to study the exterior, or exhaust flow, contamination prospects of the biowaste resistojet and how the operating conditions of pressure, temperature and composition affect the contamination prospects. The Task III effort comprised approximately ½ professional man-year of effort. This document is the summary final report on work conducted under Task III. Details on the work summarized in this report are available in the monthly technical progress letters.

1.1 Study Guidelines

The study of the biowaste resistojet exhaust effects upon spacecraft was conducted within specific guidelines dictated by the interest in specific propellant sources and thruster characteristics. The level of detail which could be provided was constrained by the scope of the effort.

The biowaste propellant mixtures considered were comprised of three constituents. These were a) the Sabatier reactor effluent b) the effluent

of the cabin carbon-dioxide molecular sieve, and c) water and water vapor from various sources. The Sabatier reactor output fluid is principally methane with traces of water, nitrogen and hydrogen.

Resistojet thrusters in the range of thrust from 0.04 to 0.22 N (10-50 mlb) were to be studied. Thrusters of this size are representative of those which would be used to accomplish low thrust maneuvers on a large manned space vehicle. Thruster operating temperatures ranging from ambient to the limit of contemporary resistojet technology ($300^{o}K$ - $1600^{o}K$) were to be examined parametrically to determine contamination compatible regimes.

Maximum use of extant analytical models for jet exhaust flows was to be made. Extrapolations or modifications of existing analyses, primarily for inviscid flow, were to be used as much as possible to be consistent with the scope of effort to be applied.

1.2 Study Scope and Objectives

The objective of this analytical study was to define the operational limits on the thruster and propellant supply subsystems of a biowaste resistojet propulsion system to minimize, or eliminate, jet exhaust interactions. The intent was to determine which mixture compositions, thrusts, pressures and resistojet operating temperatures caused the jet exhaust flow to exhibit deleterious contamination effects on the spacecraft operations. The effects of interest were: extreme jet spreading, condensate particle generation in and impingement by the jet, and the potential for condensation on adjacent surfaces. These predicted operating constraints could then be used to select test conditions for jet exhaust flow simulation tests to illustrate the expected effects and better define limits. This data, when verified, would be used in setting propellant management subsystems operating parameters. The data could also be used to select experimental parameters for a flight test

demonstration.

To accomplish the above objective, the scope of the study included the following:

A. The performance of a brief literature search to assess the applicability of extant inviscid plume analyses to the viscous resistojet flow.

B. The preparation of a summary of prior experience in spacecraft systems of contamination effects of jet flows on instruments and equipment.

C. The development of analytical models of the two phase viscous jet in sufficient detail to predict jet properties as a function of resistojet operating parameters.

D. The exercise of the models developed to determine the range of parameters for which potentially contaminating exhaust effects are predicted.

E. The evaluation of ground test facility requirements to simulate the predicted exhaust effects.

F. The definition of general guidelines for a flight experiment to substantiate the analyses and ground test results regarding contamination effects.

G. The summarization of the results and conclusions of the analysis and the preparation of specific recommendations.

To implement this scope of study activity the contract was organized into four (4) major task areas to be conducted sequentially.

1.3 Task Descriptions

The four tasks of the study, exclusive of the documentation, were topically divided as follows. This nomenclature of the tasks is consistent with the contract schedule.

1.3.1 Literature review and problem survey (Task 4.1)

This task included the survey of the literature pertaining to exhaust plume descriptions in two-phase, low Reynold's number flow. Properties examined included jet density, flow velocity magnitude and direction, condensation criteria, and two phase (particulate-gas) flow dynamics. Also examined were the literature entries related to past ground test and spacecraft flight experience with exhaust plume contamination.

1.3.2 Analysis and modeling (Task 4.2)

In this task the various models required were developed. These included:

a. A low Reynold 's number plume spreading model.

b. A thermodynamic model for the inception of biowaste condensation in the exhaust.

c. A model of condensate trajectories in the jet plume.

d. A model predicting the conditions for the accumulation of condensed biowaste exhaust on impinged spacecraft surfaces.

e. A model describing the lifetime of the biowaste resistojet exhaust products in the vicinity of the spacecraft.

1.3.3 Exhaust contamination limits on biowaste resistojet operating parameters (Task 4.3)

In this task the models developed in the preceding work were exercised using the parameters and constraints of pressures, thrust, temperature, and mixture compositions to describe the limits which would permit resistojet functioning with minimal contaminating effects on the spacecraft.

1.3.4 Experiments definition and criteria (Task 4.4)

Using the results of the prior work, the recommendations of facility requirements for ground test verification of the predicted contamination were developed. Also, comments in the objectives of a flight test experiment to further examine the jet contamination on spacecraft systems were developed.

1.4 Schedule of Task Performance

The chronological sequence of task performance is presented in Figure 1. The detail reporting of the task activity was accomplished via the monthly technical progress reports required under the contract. The monthly report containing detail of specific tasks is also indicated in Figure 1. This Task III effort was initiated on October 1971 and continued through May 1972.

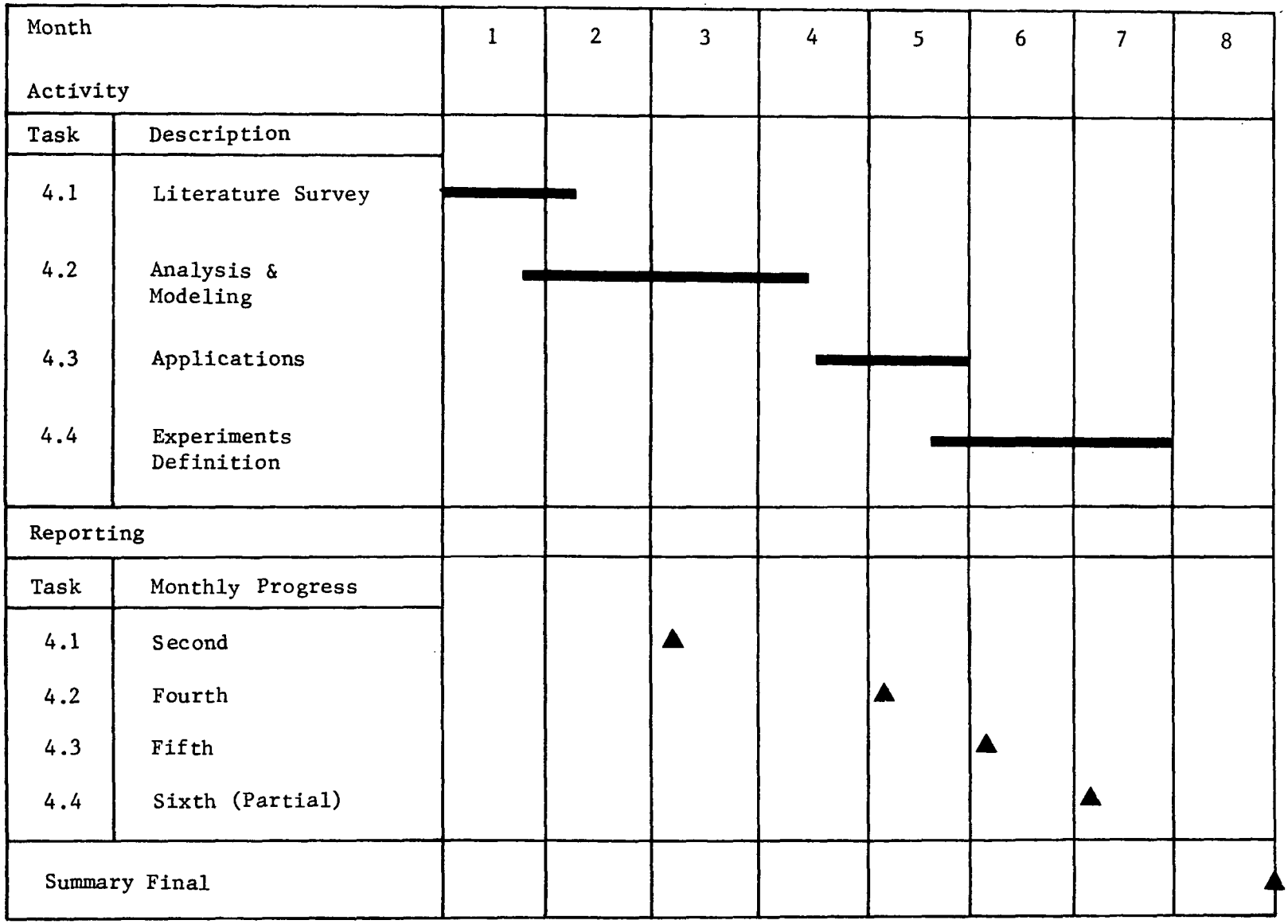

Figure 1. Study Performance and Milestone Schedule.

2.0 TECHNICAL SUMMARY

2.1 Literature Review and Problem Survey (Task 4.1)

In this task, the literature related to spacecraft contamination by rocket effects and that of jet plume analyses were surveyed. A computer search of the literature was conducted based upon key subject indices. Approximately 100 entries were evaluated. A listing of the key bibliography is presented in Section 5.0. In addition, telephone and personal interviews were conducted with investigators in these fields. Mr. Warren Lyon, of Hittman Associates, was interviewed at length. Mr. Lyon has been the principal investigator on NASA-Goddard Space Flight Center supported work on spacecraft-rocket contamination effects. Additional information was obtained from the Skylab Program staff, both at NASA-Marshall Space Flight Center, Langley Research Center and at the Martin-Marietta Corporation, Denver Division. NASA - Jet Propulsion Laboratory was also contacted to relate Ranger, Mariner and Surveyor experiences in this area.

A compendium of flight and ground simulation test experience with spacecraft contamination, both intentional (rocket impingement tests) and unexpected (flight and ground test anomalous events). This summary of prior experience is presented in Figure 2. A review of this data reveals that only the Apollo and Gemini window deposits could be traced to propulsion sources. The other examples of contamination could be related to propulsion events, but the data is inconclusive. The Apollo and Gemini rockets were conventional chemical bipropellants and do not directly relate to the biowaste resistojet. Electric propulsion jets in SERT spacecraft did generate some effects on the solar array, but these metal ion plumes are similarly unrelated to the resistojet and are not included.

FIGURE 2

PRIOR HISTORY OF SPACECRAFT CONTAMINATION EFFECTS

PROGRAM	FLIGHT GROUND TEST	INSTRUMENT SENSOR	EFFLUENT SOURCE/ TYPE	OBSERVED EFFECTS	PROBABLE CAUSE	REFERENCE
Nimbus II III	Flight	High Resolution Infrared Radiometer	Unknown. Possible silicon oil from thermal vac tests.	Lead selenide detector temp. rise to 208.5°K (13°C above control point), N-II HRIR didn't operate as expected. N-III worked 2 days then temp. rise. Subsequent attitude perturbation brought system back on for short periods then temp. rise.	Coating of cold spot (195°K) with ice changed α/ε and altered heat transfer. Subsequent attitude changes let sun boil-off coating and temporarily resume operation.	McNaney, J.J., etal, "Nimbus II, Flight Evaluation and Engineering Report, Launch through Orbit 5275," TN D-4881, Feb. 1969, NASA. McNaney, J.J., "Nimbus II Monthly Flight Evaluation Report Number 3, 14 June to 13 July, 1969 Orbits 800-1200," 69 SD 4338, Aug. 8, 1969, General Electric, Philadelphia, Pa.
Nimbus IV	Flight	Filter wedge spectrometer	Unknown. Possible outgas from multi-foil insulation or gas jets. Possible water-oil, water-polymer icing from outgas of insulation, oils, & materials specifically adhesives.	Degraded spectral measurement; shorter wavelength regions partially degraded, longer regions completely obscured. Ice absorption bands appeared to be in 1.2 to 2.4 region indicating water icing on 176°K sensor for 2 months at least.	Placement of detector in high outgas region. Probable deposition of outgas on cold area. Deposit probable water-oil or water-polymer compound since pure ice would sublime. Adhesives, oils & plasticizers suspected	Goldberg, I.L., "General Guidelines to Cooler Designs to Prevent Degradation," Memorandum, Aug. 11, 1970,GSFC. Scialdone, J.J., "Analysis of Filter Wedge Spectrometer (FWS) Degradation and Recommendations for Cooler Design," Memorandum, Sept.8,1970,GSFC.
ISIS-A	Ground Solar Thermal Vacuum	General outgas using gas chrom. and I.R..	Thermal vac-IR showed methyl siloxane and phthalate esters predominated on test plate, some aliphatic H/C. Solar vac-IR analysis of test plate showed methyl phenyl siloxanes and aliphatic H/C predominate,	Not less than 20 compounds identified by CC on test panels could have coated flight craft. GE RTV 115 used to adhere solar cells to solar panels substrate continuously bled low MW silicone oil with or without prior vac exposure. Expected yield of 3.2g/100g adhesive could have coated most of craft ex-	Poor choice of silicone materials and adhesives from outgas standpoint.	Goldsmith, J.C., "Summary of ISIS-A Spacecraft Outgassing Data, "SP912-0027, Mar. 1969, Sperry Rand Corp., GSFC, Greenbelt, Md. Nelson, E.R., J. Haynes, and KF Plitt, "Outgassing and Condensable Oils from Adhesive in ISIS Solar Panels, Memorandum

FIGURE 2 (CONT'D)

PRIOR HISTORY OF SPACECRAFT CONTAMINATION EFFECTS

PROGRAM	FLIGHT GROUND TEST	INSTRUMENT SENSOR	EFFLUENT SOURCE/ TYPE	OBSERVED EFFECTS	PROBABLE CAUSE	REFERENCE
cont'd. from prior page			some esters, and aromatic H/C present. Probably from epoxy adhesives (such as FM-1000), RTV's and silicone oils or grease outgassing.	terior under space conditions.		from Materials R&D Branch, GSFC, Feb.8,1967,GSFC.
OAO-A2	Ground Solar-Thermal Vacuum	UV Absorption spectroscopy (diagnostic)	Dimethyl silicone probably from combined outgassing of RTV,LTV, and other silicone resins. Also a complex series of H/C that could have come from poor cleaning of oils and lubricants and a phthalate ester from a single type of plasticized polymer.	Deposits on star tracker, near foil insulation vents, and electronics boxes. The phthalate ester shows strong UV absorption from 200 to 250 millimicrons (peak 204 m) which could have affected experiment optics.	Used cold traps instead of continuous pumping so vapors were not removed from cell. Also improper venting of trapped outgas prolonged transient and allowed deposits.	Nelson,E.R. F. Gross, and J.J. Park, "Analysis of OAO A-2 Outgassing Deposits, "Memorandum from Materials R&D Branch, GSFC, June 17,1968, NASA.
OGO II, III,IV also Exp. XVII	Flight	Neutral Mass Spec.	Probable neutral particle, water-icing on 170°K probe	OGO II and OGO IV experienced a drop in particle level of 1-2 orders of magnitude within 40 days of launch, then leveling to a drop of one order of magnitude in approximately 200 days. On OGO IV MS indicated mass no.18 (water) rose to peak of 4 x $10^8/CM^3$ in approx. 100 mins. after opening of instrument then dropped into noise level of 3 x $10^6/CM^3$ after 90 days. Spacecraft outgassing of water vapor dominated OGO III MS; with variation in H_2O level per orbit, but level decreased with time.	Water outgas condensate, estimated density of outgas 10^3 times ambient for OGO III.	McCulloch,A.W., "H_2O Environment in Vicinity of Satellites" Memorandum,Sept.8,1970,GSFC Hinton,B.B., et al,"Neutral Particle and Positive Ion Data Obtained from OGO-C," Trans. AGU, 48,1967,pp. 74-75. Grenda, R.,S. Neste, and R. Soberman, "ContaminantParticle Trajectories Near a Spacecraft" COSPAR, Plenary Meeting, May 9-21, 1968, A68-31916.

FIGURE 2 (CONT'D)
PRIOR HISTORY OF SPACECRAFT CONTAMINATION EFFECTS

PROGRAM	FLIGHT GROUND TEST	INSTRUMENT SENSOR	EFFLUENT SOURCE/ TYPE	OBSERVED EFFECTS	PROBABLE CAUSE	REFERENCE
RAE-A Satellite	Ground Thermal Vacuum	Analysis of Cold Trap	Honeycomb adhesive (FM-1000), no pump oil	Analysis of cold trap showed a complex mixture of aliphatic and/or alicyclic H/C (perhaps a high boiling petroleum fraction lub. oil), dimethyl and phenylmethyl silicone (most likely from RTV or other resins), and phthalate esters and aliphatic ketones (plasticizer from polymers).	Poor choice of adhesives and plasticizers from outgas standpoint	Nelson,E.R., "Outgassing During Thermal Vacuum Tests on RAE-A Satellite," Memorandum, GSFC Materials R&D Branch, April 12, 1968, NASA.
Mariner IV, V	Flight	Canopus Sensor	Bright particles assumed to be dust	Lost star lock 20-40 times in flight. Violent responses in roll error channel during motor burn and explosive valve firings	Bright particles reflecting sun confused sensor. Most often following S/C firings or deployment vibrations. Mariner VI, VII changed sensitivity levels of sensor to improve. Probably environmental dust from fab.	Goss, W.C.,"The Mariner Spacecraft Star Sensors," Applied Optics, Vo. 9, No. 5 May 1970, pp. 1056-1067.
OGO-VI	Flight	Quartz crystal microbalance	Epoxies used in solar panels, oils absorbed during vacuum tests, and volatile gases such as O_2, N_2, CO_2, and H_2O (g).	Contaminant build-up on Al and Au surfaces for 5 months. Slow return to normal due to upper atmosphere cleaning effects.	Outgas from solar panel adhesive and residual oils.	McKeown, D., and W.E. Corbin, Jr., "Space Measurements of the Contamination of Surfaces by OGO-6 Outgassing and their Cleaning by Sputtering and Desorption," Paper No. 7, Gaithersburg, Md., 1970.
Mercury	Flight	Window optics (post flight) analysis	Outgassed Material from launch shroud	Window coatings obscured view	Nose cone outgas, windows covered on later Gemini launches to prevent coating.	Blome, James C., and Bruce E. Upton, "Gemini Window Contamination Due to Outgassing of Silicones, "contained in The Effects of the Space Environment on Materials, Vol. II, 11th National Symposium and Exhibit, SAMPE, St. Louis, Apr. 1967 (A67-29555).

FIGURE 2 (CONT'D)
PRIOR HISTORY OF SPACECRAFT CONTAMINATION EFFECTS

PROGRAM	FLIGHT GROUND TEST	INSTRUMENT SENSOR	EFFLUENT SOURCE/ TYPE	OBSERVED EFFECTS	PROBABLE CAUSE	REFERENCE
cont'd. from prior page						Bonner, George P., et al, "Post-Flight Optical Examination of the Right-Hand and Left-Hand Windows of Gemini Missions IV, V, VI and VII "NASA TND-4916 (N69-13232), Dec. 1968.
Gemini	Flight	Window optics (post flight) analysis	Motor ablation (refrasil) propellant impurities waste dumps, window sealer, paint pigment	Windows coated by an oil-like deposit. S/C surface pitting by thruster debris, gouging by cohesive particles, and chemical interaction with corrosive materials.	Long term outgas and propellant use also urine dump.	Baurer, T., et al, "External Spacecraft Contamination Modeling and Countermeasures," Paper No. 5, Gaithersburg, Md. 1970. Blome, James C., and Bruce E. Upton, "Gemini Window Contamination Due to Outgassing of Silicones, "contained in The Effects of the Space Environment on Materials, Volume II, 11th National Symposium and Exhibit, SAMPE, St. Louis, Apr. 1967 (A67-29555). Bonner, George P., et al, "Post Flight Optical Examination of the Right-Hand and Left-Hand Windows of Gemini Missions IV, V, VI, and VII" NASA TND-4916 (N69-13232), Dec. 1968. Hallgren, D.S., and C.L. Hemenway, "Direct Observation of Particulate and Impace Contamination of 'Optical' Surfaces in Space," COSPAR, Plenary Meeting, May9-21, 1968 (A68-31919)

FIGURE 2 (CONT'D)
PRIOR HISTORY OF SPACECRAFT CONTAMINATION EFFECTS

PROGRAM	FLIGHT GROUND TEST	INSTRUMENT SENSOR	EFFLUENT SOURCE/ TYPE	OBSERVED EFFECTS	PROBABLE CAUSE	REFERENCE
Apollo Unmanned (I-VI) Manned (XI)	Flight	Window optics (post flight analysis)	Rocket outgas RCS solder flux igniters, pyros RTV	See Gemini Effects	General outgas and propellants	Baurer, T., et al,"External Spacecraft Contamination Modeling and Countermeasures," Paper No. 5, Gaithersburg, Md., 1970. Arnett, G.M., "Lunar Excursion Module RCS Engine Vacuum Chamber Contamination Study," TMX-53859, MSFC, July 8, 1969, NASA.
Viking	Ground Test flight spec	GC/MS	Organic construction materials outgas, fuel contaminants	Anticipate confusion of instrument at levels above 0.1 ppm organic contamination in samples.	Planning stage, restrictions on organic materials and processes usage, sealed GC/MS unit and sample path. Fuel purity requirement.	LRC - Viking Project Office, L.P. Daspit, Jr. "Viking 75 Project Lander Science Contamination Control Plan," NASA/LRC, Viking Project Office, PL-3701045. "Viking Mandatory Materials List," Martin Marietta Corporation, Denver, Colorado, Drawing No. 83703040205.

FIGURE 3

PROPULSION EXHAUST CONTAMINATION STUDIES

JET SOURCE	TARGET	CONDITIONS	EFFECTS	AGENCY
25 lb. Hydrazine	Thermal Paint Solar Cells Optics	Vacuum (400,000 ft.) cryo-pumped direct impingement pulses	No appreciable influences	AFRPL Martinkovic
Solid Retro	Thermal Paint	Vacuum, U.V. Light	Increased solar absorbtance particularly with U.V. exposure	Hughes A. C. (MSFC)
Gemini RCS	Exposure Plates	Flight Coupons Gemini 9, 12	Particulate contam-ination splatters & gouges attributed to RCS exhaust	S.U.N.Y. (MSC)
Model N_2O_4/MMH	Calorimeters force gages	Vacuum 325,000 ft. 20 MSEC pulse	Heat and pressure forces on targets	Cornell Aero-lab (MSFC)
SIVB Retro Solid	Solar cells laser beam	Vacuum 130,000 ft.	26% loss of solar cell performance 20% laser attenu-ation	ARO
N_2O_4/MMH	Target glass strips with NaCl strate	Vacuum, pulse mode	Trace metals parti-culate on targets, also nitrates	NAR

The principal outcome of the spacecraft contamination survey is that water and water-bearing compounds have caused film deposits to occur on spacecraft sensors held at low temperature. This information was of use in the later analyses of this study. Conditions for condensation of water, carbon-dioxide and methane were evaluated, and the results appear in Section 2.3.2.

Review of the jet plume characterization analyses indicated that most analyses are available for inviscid jets only. The small size and flow rate of the biowaste resistojet of interest place the flow well into the viscous regime. This required that the inviscid jet analysis be analyzed to develop viscous jet perturbations of the analyses that are available. The general comment upon the available analysis is that they treat the chemical thermodynamics of the jet in great detail and are complicated by this feature. The resistojet operating regime (residence time and temperature) is such that little or no chemical activity is predicted to occur for the compounds of interest to this study. The bibliography of Section 5.0 contains numerous entries describing the inviscid jet flow analyses.

2.2 Analysis and Modeling (Task 4.2)

2.2.1 Propellant gas property analysis

Before the analysis of viscous plume exhaust processes could be initiated, it was necessary to establish the vapor mixture properties of the biowaste propellants of interest. Prior work on the biowaste resistojet system preliminary design and description by McDonnell Douglas Corporation has identified six candidate vapor mixtures. The transport properties of these mixtures were described in MDAC Bulletin 16 of NAS1-10127 by Page of Advanced Rocket Technology. One property not tabulated was the gas

mixture specific heat ratio (c_p/c_v). This property is significant for all plume expansion processes, both ideal and viscous.

Using ideal gas theory for gas mixtures, and the physical properties for the constituents, the specific heat ratio for the gases was calculated. The results are presented in Table 1 for four (4) gas temperatures, namely 300°K, 500°K, 1000°K and 1600°K. These temperatures were selected as being representative of: ambient vent, warm vent, medium heated vent, and high temperature vent, respectively. Estimates for methane containing mixtures are not presented at 1600°K because of past experience with disassociation of methane above 1000°K. The composition of the candidate mixtures is presented in Table 2 for reference.

The data of Table 1 was used in subsequent analysis of condensation, pluming and nozzle flow. A small value of the ratio indicates a high heat capacity and, therefore, a greater capacity to turn from the nozzle axis in Prandtl-Meyer flow expansions. Note that at ambient temperature almost all the mixtures display a value of approximately 1.3. This is representative of an ideal gas of 3 or more atoms without appreciable excitation of internal degrees of freedom. At elevated temperatures the specific heat ratio reduces due to excitation of these internal degrees of freedom, and the variation increases among gases due to their differing molecular composition and structure. As the plume expands, the internal degrees of freedom "freeze" and γ increases to a theoretical limit of 1.67. In subsequent pluming analyses, an average was used.

TABLE I

Specific Heat Ratio For Candidate Biowaste

Resistojet Propellant Mixtures

Propellant Type	Source	Temperature			
		300°K	500°K	1000°K	1600°K
A	CO_2 Sieve Output	1.29	1.23	1.19	1.17
B	Sabatier Output	1.30	1.25	1.17	N/A
C	Mixed A & B	1.30	1.25	1.18	N/A
D	Water	1.33	1.32	1.29	1.26
E	Mixed A & B	1.30	1.24	1.18	N/A
F	Mixed B & C	1.31	1.28	1.21	N/A

* See Table 2 for compositions

TABLE 2

Propellant Descriptions

Propellant		Source	Composition	
Type	Nominal		Species	Mole fraction
A	CO_2	Molecular sieve waste output. (Scrubbed from spacecraft atmosphere)	CO_2	0.984
			N_2	0.012
			O_2	0.004
B	CH_4	Sabatier waste output	CH_4	0.917
			CO_2	0.054
			N_2	0.014
			H_2O	0.015
C	CO_2 & CH_4	Combined outputs A and B	CO_2	0.405
			CH_4	0.572
			N_2	0.012
			O_2	0.001
			H_2O	0.010
D	H_2O	Water recovery	H_2O	1.000
E	CO_2 & CH_4	Combined outputs A and B in stoichiometric ratio of nominal propellants	CH_4	0.488
			CO_2	0.488
			N_2	0.012
			O_2	0.004
			H_2O	0.008
F	H_2O	Combined outputs B and C in stoichiometric ratio of nominal propellants	CH_4	0.483
			CO_2	0.028
			N_2	0.007
			H_2O	0.483

2.2.2 Modeling viscous expansion processes

The objective of this study is to predict resistojet expansion characteristics as the propellant properties vary due to temperature, pressure and composition. A key departure of the flows in the resistojet from classical inviscid jet flow is that viscous effects dominate the nozzle expansion process. This is evident from the referenced experimental correlations done by Page of Advanced Rocket Technology for McDonnell Douglas Corporation in Bulletin No. 16. See Figure 4. The discharge coefficient (flow rate reduction) and the specific impulse were correlated with a viscous parameter (G) which is a function of Reynolds number of the nozzle flow. It is the purpose of this study to use this experimental basis to predict flow properties. In keeping with the scope of the study, the approach to be used is that of perturbing the ideal jet solutions using parameters derived from experimental thruster tests. The viscous parameter G(Re) is defined as

$$G(Re) = \frac{(\dot{m}/A^*)_{eff} F}{\mu_{TF} I_{SPF_\infty} g_o}$$

where: $(\dot{m}/A^*)_{eff}$ = effective mass flux at throat

F = thrust

μ_{TF} = dynamic viscosity at chamber T

I_{SPF_∞} = ideal specific impulse at infinite expansion

g_o = gravitational conversion factor.

Typical biowaste resistojet thrusters of interest exhibit values of G from 10^5 to 10^8 . The wide range displayed arises from the need to treat varying compositions, temperatures, thrusts and pressures.

An ideal (inviscid) nozzle exhibits isentropic flow. This results in C_D and impulse ratio of unity. The inviscid flow in the nozzle was approached from entropy considerations as being polytropic in behavior. The equation of the gas state for this assumption is

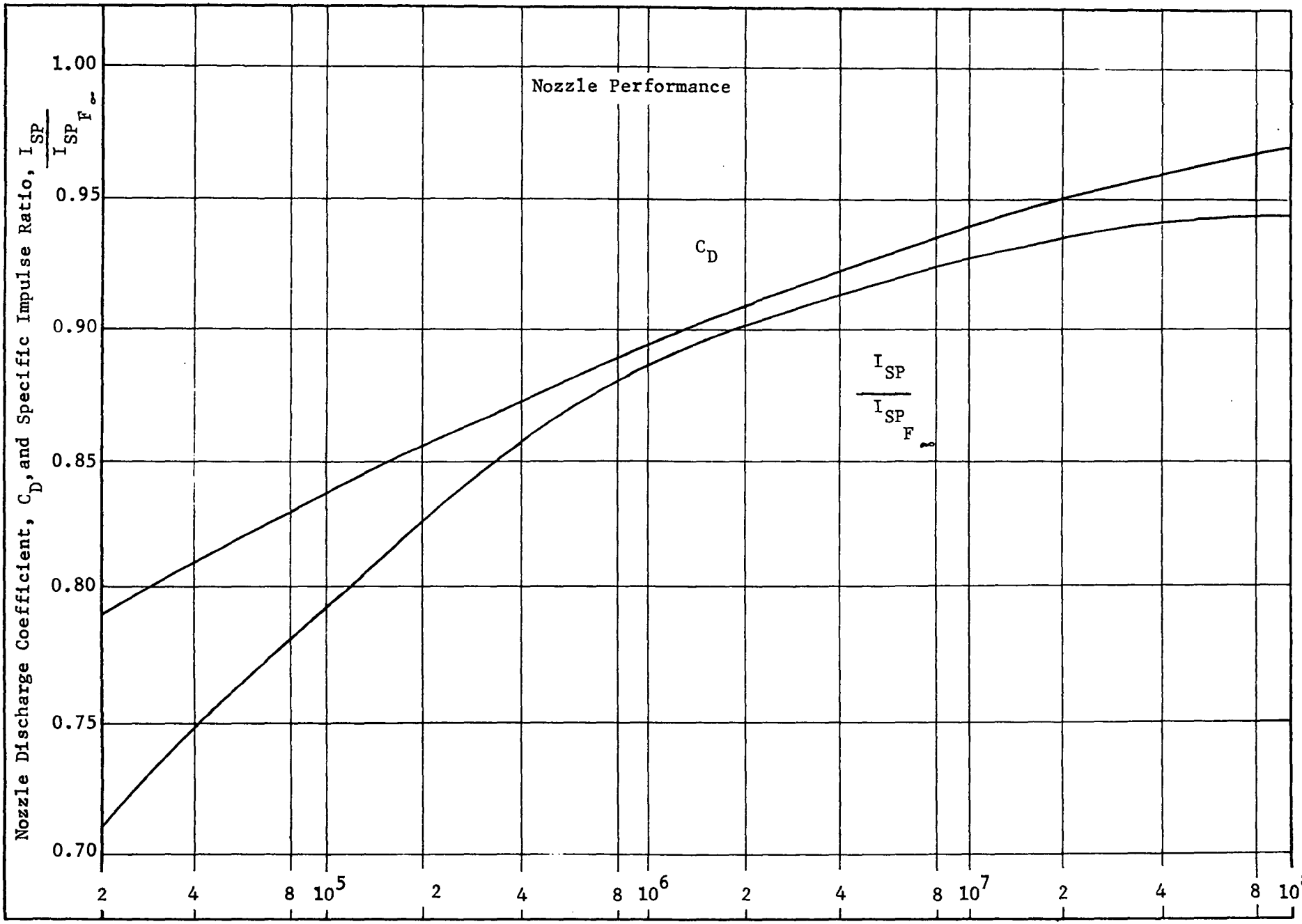

Figure 4. Reynolds Number Function, $G(RE\#_D)$

$$P/\rho^n = \text{constant}$$

Ratioing the corresponding relations for polytropic flow mass flux and isentropic flow mass flux results in the relation

$$C_D = \sqrt{\frac{n-1}{n+1}} \left(\frac{2}{n+1}\right)^{\frac{1}{n-1}} \sqrt{\frac{\gamma+1}{\gamma}} \left(\frac{\gamma+1}{2}\right)^{\frac{1}{\gamma-1}}$$

Using the experimental data for C_D per Figure 4 and the γ data from Table 1, the n is implicitly defined from the above. A linear expansion of the preceding function was performed to achieve an approximation for rapid, simple calculation. This function is:

$$C_D \cong 1 - \frac{\gamma}{\gamma-1} \ln \frac{+1}{2} \left(1 - \frac{\gamma}{n} \frac{n-1}{\gamma-1} + \ldots .\right)$$

In this function, γ is always greater than n by entropy considerations, and C_D is therefore less than unity. This function was plotted and is presented in Figure 5 for C_D versus γ-n. The variation from a linear function for all γ of interest was found to be less than 0.01 on the C_D axis. An interesting feature of the analysis, which is consistent with Page's correlation referenced previously, is that there is not strong direct dependence on γ itself. For all of the gas states of interest the above C_D vs. (γ-n) is virtually independent of γ. The linear graph of Figure 5 is used as follows. Given resistojet design features, the G(Re) function may be computed. From this the correlation of Figure 4 can be used to estimate C_D, which in turn gives an entry into Figure 5 for the equivalent n for the nozzle expansion process knowing γ of the gas. Once n is determined then other properties of the flow can be estimated, using the equation-of-state relation.

One such property of interest is the relation between area ratio and temperature. This can be derived from the preceding to yield

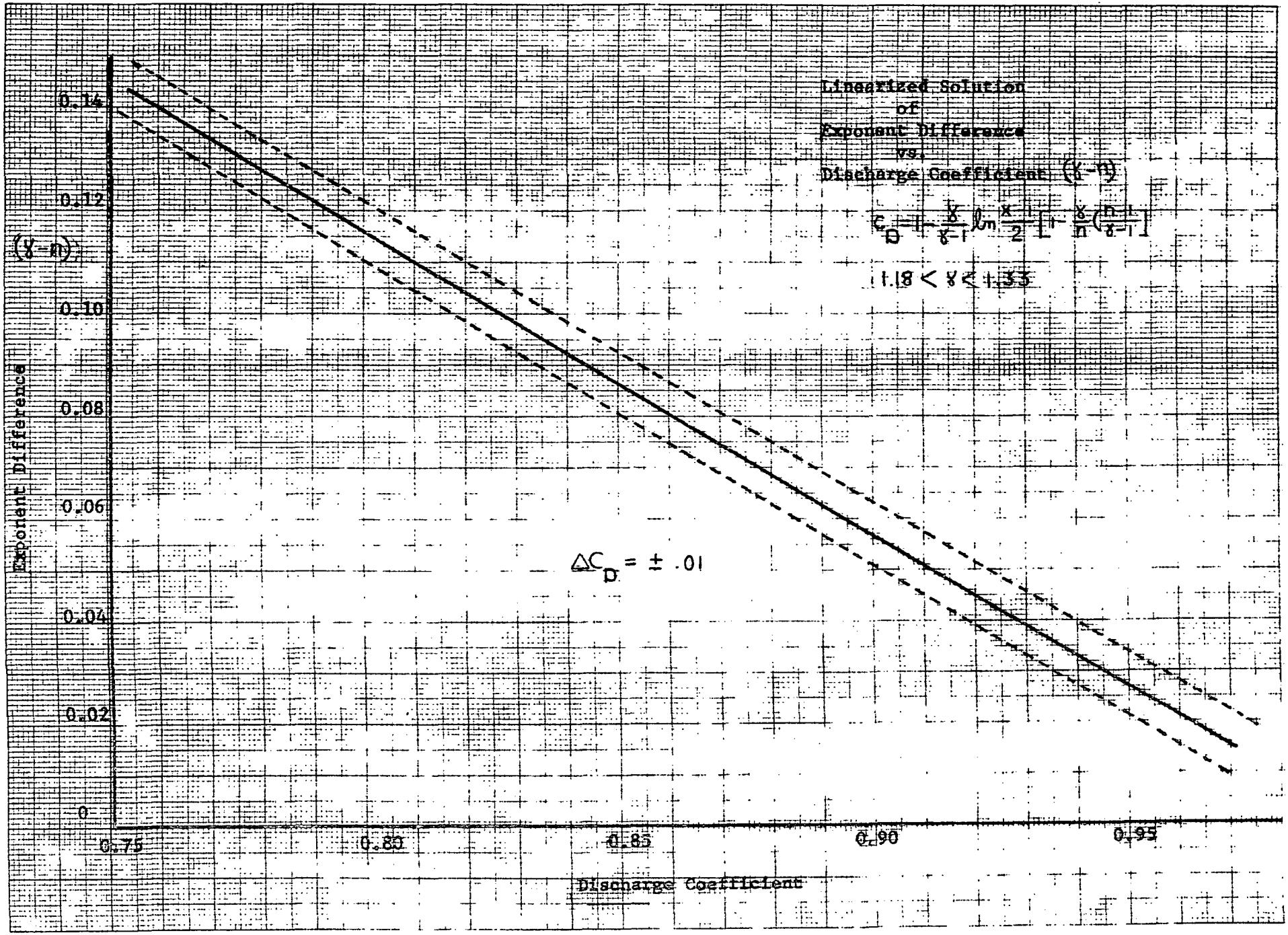
Linearized Solution
of
Exponent Difference
vs.
Discharge Coefficient $(\gamma-n)$
$C_D = 1 - \frac{\gamma}{\gamma-1} \ln \frac{x}{2} \left[1 + \frac{\gamma}{n}\left(\frac{n+1}{\gamma-1}\right)\right]$
$1.18 < \gamma \leq 1.33$
$\Delta C_D = \pm .01$
Exponent Difference
$(\gamma-n)$
0.14
0.12
0.10
0.08
0.06
0.04
0.02
0
0.75
0.80
0.85
0.90
0.95
Discharge Coefficient

Figure 5

$$\left(\frac{A_t}{A_x}\right)^2 \frac{n-1}{n+1}\left(\frac{2}{n+1}\right)^{2/n-1} = \frac{T_o/T_x - 1}{\left(\frac{T_o}{T_x}\right)^{\frac{n+1}{n-1}}}$$

where A_t/A_x is the nozzle area expansion ratio and T_o/T_x is the ratio of chamber stagnation temperature to exit static temperature. The area ratio at various temperature ratio is presented in Figure 6 , for a range of biowaste gas parameters. The trend of Figure 6 is that for low values of n, the temperature ratio is correspondingly low at fixed area ratio.

2.2.3 Free expansion

Once the jet exits the nozzle, the flow will relax to an isentropic expansion since the wall friction effect will be absent. Neglecting the region where flow relaxes from the viscous interior flow to the exterior flow, the exterior flow can be approximated from inviscid theory. This is an averaging type of approximation since in the real case there will be velocity gradients associated with the initial velocity distribution present at the nozzle exit.

The approach used in predicting the plume shape and flow characteristics is that developed by Hill and Draper. In this approximation to the flow the farfield of the jet is assumed to be radial source flow with the stream density (ρV) varying as $1/r^2$ from the nozzle apex. In the very near vicinity of the nozzle, the flow prediction may not be totally accurate, but the trends are consistent. The mass flux per unit solid angle is

$$\frac{\dot{dm}}{d\Omega} = \rho V r^2$$

The mass flux $\frac{\dot{dm}}{d\Omega}$ shows a very rapid decay from the axial station in the exact solutions of the flow developed in method of characteristics solutions.

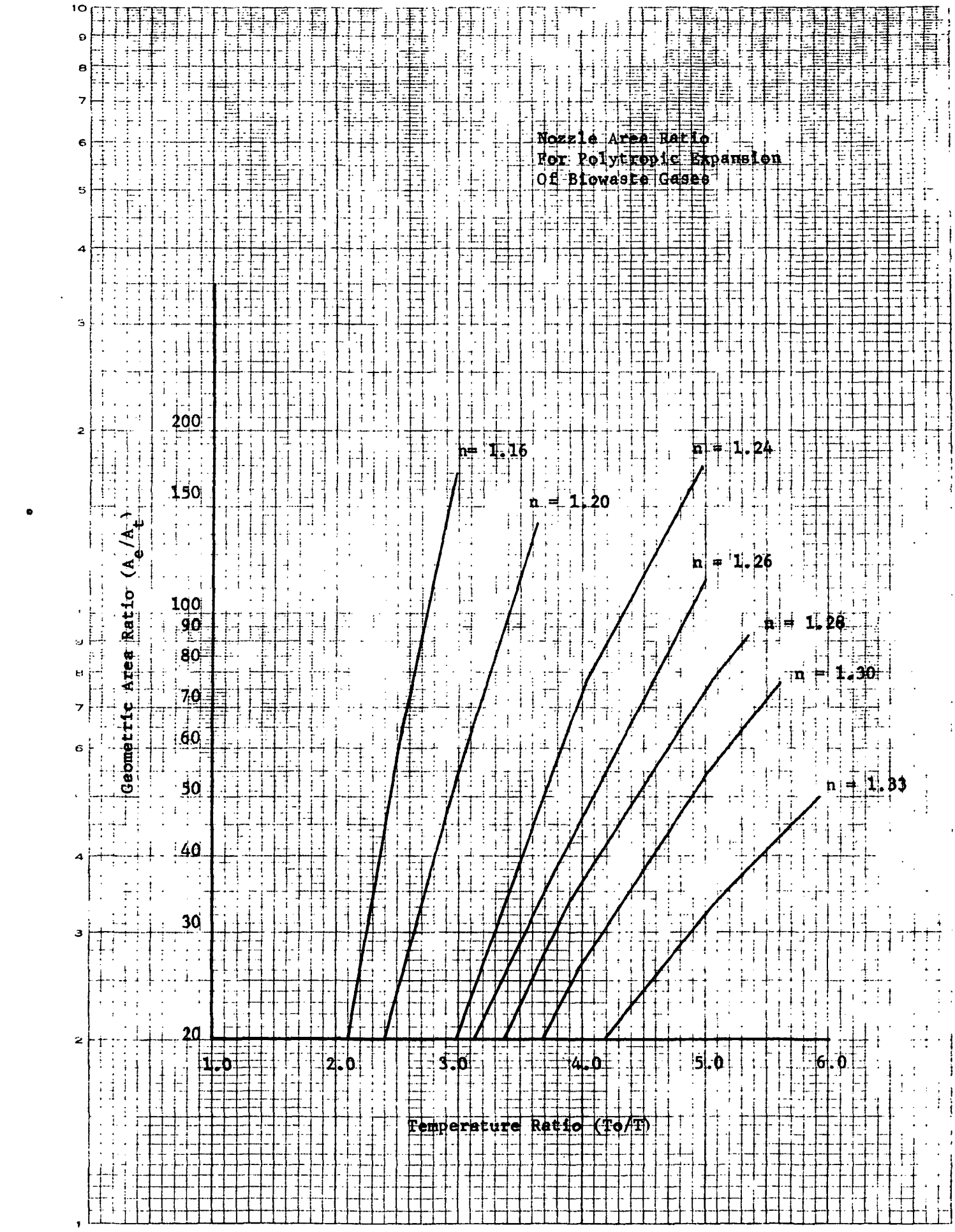
Nozzle Area Ratio
For Polytropic Expansion
Of Blowaste Gases
Geometric Area Ratio (A_e/A_t)
Temperature Ratio (To/T)
n= 1.16
n = 1.20
n = 1.24
n = 1.26
n = 1.28
n = 1.30
n = 1.33
200
150
100
90
80
70
60
50
40
30
20
1.0
2.0
3.0
4.0
5.0
6.0

Figure 6

A one parameter function has been developed to approximate this decay by Hill and Draper

$$\left(\frac{d\dot{m}}{d\Omega}\right)_\theta \Big/ \left(\frac{d\dot{m}}{d\Omega}\right)_{\theta=0} = f(\theta) = \exp\left[-\lambda^2(1-\cos\theta)^2\right]$$

The value of λ, the parameter must be determined from the solution of the mass and momentum conservation equations. This results in the following for the λ solution

$$\lambda = \frac{1}{\pi^{1/2}\left(1 - \frac{I_s}{I_{s\infty}} V/V_{MAX}\right)}$$

In this function, the $I_s/I_{s\infty}$ ratio can be obtained from Figure 4 knowing the flow G(Re) function. V/V_{MAX} is the ratio of gas velocity to the ideal, one dimensional, infinite expansion velocity. In the limit of high expansion, this ratio approaches unity, and the corresponding λ is referred to as λ_∞. Note that for each isodensity contour, there is a corresponding V/V_{MAX} and, therefore, λ, which describes each contour, as will be shown.

The ratio of V/V_{MAX} is given by the following.

$$V/V_{MAX} = \sqrt{1 - T/T_o} = \sqrt{1 - \frac{T_e}{T_o}\left(\frac{\rho}{\rho_o}\right)^{\gamma-1}\left(\frac{T_o}{T_e}\right)^{\frac{\gamma-1}{n-1}}}$$

In this function T/T_o is the ratio of stream static temperature to total temperature, and T_e/T_o is the corresponding ratio for nozzle exit conditions. These dual functions are required because in expansion, the gas first expands in the nozzle polytropically. The ratio T_e/T_o is obtained from Figure 6 for the appropriate flow parameters and area ratio. The ratio ρ/ρ_o is selected as the value for the desired isodensity contour of the plume.

Returning to the plume description problem, the preceding analyses can be combined to describe the plume isodensity contours. The relation derived is

$$\left(\frac{r}{r_e}\right)^2 = \frac{C_D}{\pi}\sqrt{\frac{\gamma-1}{2}}\left(\frac{2}{\gamma+1}\right)^{\frac{\gamma+1}{2(\gamma-1)}}\frac{\rho_o}{\rho}\frac{A_t}{A_e}\frac{V_{MAX}}{V}\exp\frac{-\left[\frac{(1-\cos\theta)^2}{\pi\left(1-\frac{I_s}{I_{s\infty}}V/V_{MAX}\right)^2}\right]}{1-\frac{I_s}{I_{s\infty}}V/V_{MAX}}$$

In this function r_e is the nozzle exit radius and r is the radius from the nozzle apex to the point in the plume where the isodensity contour ρ/ρ_o is described, at the angle θ. Choosing a density value, and from the previously defined parameters, it is possible to compute isodensity contours of the flow. These contours, and the assumption that the flow in the far field is radial outward at any angle θ from the axis with origin at the nozzle apex, allows computation of mass flux as a function of angle. Three typical plume plots are presented in Figures 7 through 9 for the stated parameters of biowaste resistojet interest. The results are shown comparatively in Figure 10 . Figure 11 presents plume plots for a range of G(Re) conditions. to illustrate the significant effect of viscosity in plume shape, when compared with inviscid predictions.

Among the plume properties investigated was that of predicting the flow which turns greater than 90^o, i.e. past the nozzle lip and upstream. The relation derived is

$$\frac{\dot{m}\ (\text{greater than } 90^o)}{\dot{m}\ (\text{total})} = \frac{\int_1^\infty e^{-\lambda^2 \eta^2} d\eta}{\int_0^\infty e^{-\lambda^2 \eta^2} d\eta}$$

This function is of significance when it is desired to estimate the flow which will occur on upstream spacecraft components and gives a gross measure of the severity to be expected.

2.2.4 Entrained particulate trajectories

Particulate material can be expected to be present in the biowaste resistojet exhaust. This particulate material can arise from: the condensation of vapors in the resistojet propellant mixtures, the flaking of materials of construction of the thruster system, the decomposition of methane to solid carbon, and the traces of solid salts that can be present in some of the sources of biowaste propellant. These particulates will be entrained in the

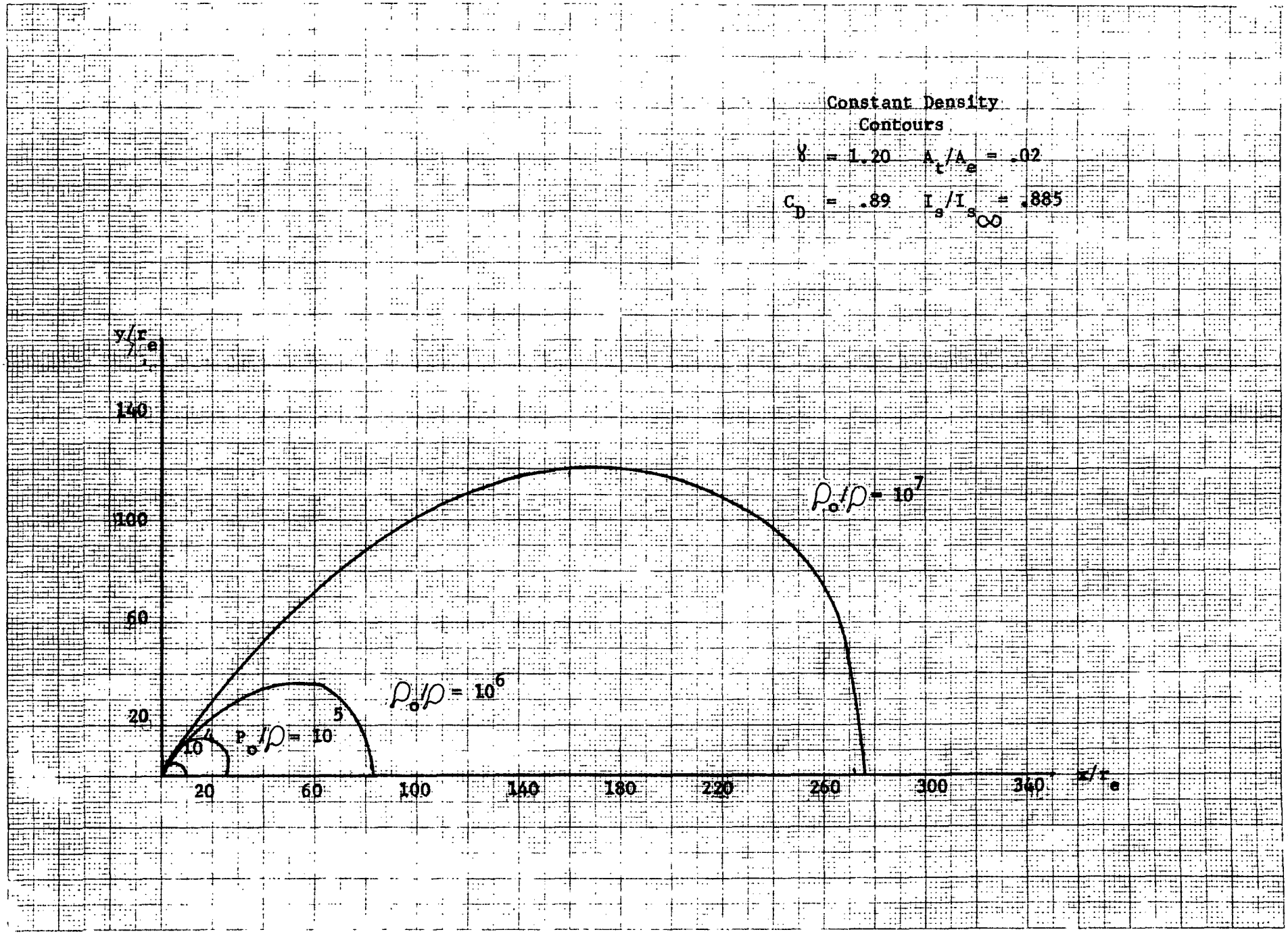
Constant Density
Contours
γ = 1.20 A_t/A_e = .02
C_D = .89 I_s/I_{s_∞} = .885
y/r_{t_e}
140
100
60
20
$\rho_o/\rho = 10^7$
$\rho_o/\rho = 10^6$
$\rho_o/\rho = 10^5$
10
20
60
100
140
180
220
260
300
340
x/r_{t_e}

Figure 7

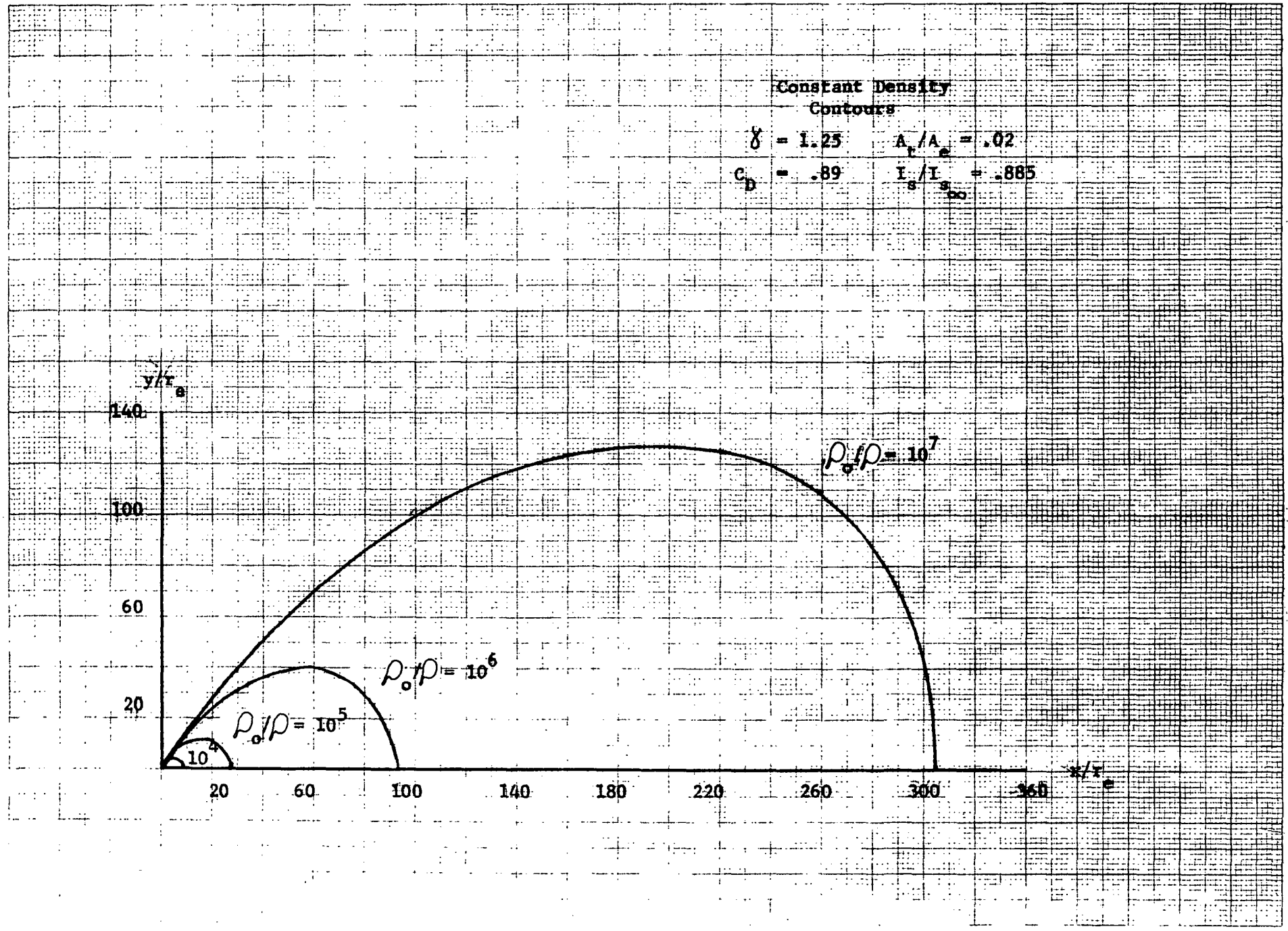
Constant Density
Contours
γ = 1.25
A_t/A_e = .02
C_D = .89
I_s/I_{s_∞} = .885
y/r_e
140
100
60
20
$\rho_o/\rho = 10^7$
$\rho_o/\rho = 10^6$
$\rho_o/\rho = 10^5$
10^4
20
60
100
140
180
220
260
300
360
x/r_e

Figure 8

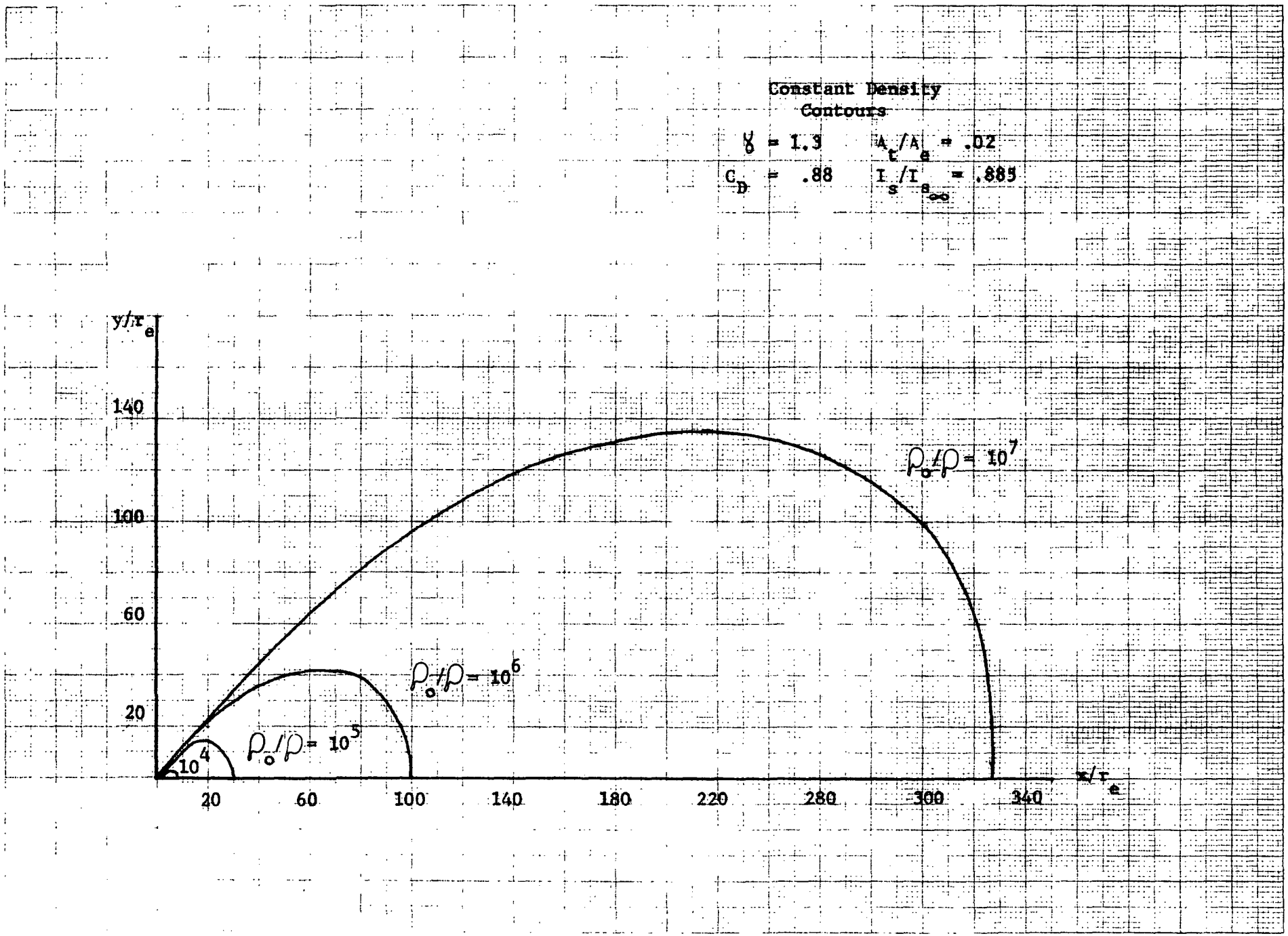
Constant Density
Contours
γ_0 = 1.3
A_t/A_e = .02
C_D = .88
I_s/I_{s_∞} = .885
y/r_e
140
100
60
20
$\rho_o/\rho = 10^7$
$\rho_o/\rho = 10^6$
$\rho_o/\rho = 10^5$
10^4
20
60
100
140
180
220
280
300
340
x/r_e

Figure 9

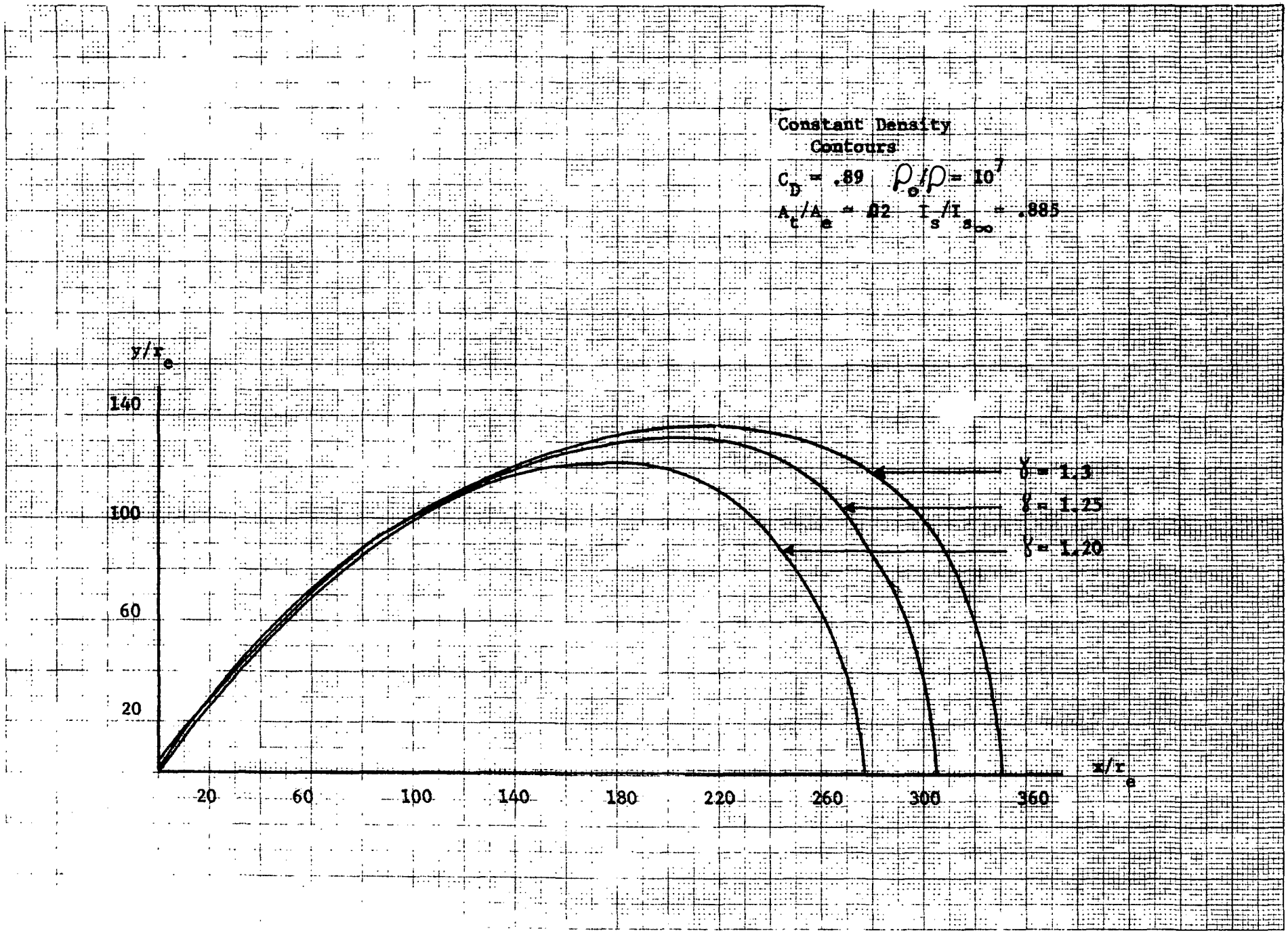
Constant Density Contours
C_D = .89 $\rho_e/\rho = 10^7$
A_t/A_e = .02 I_s/I_{s_∞} = .885
y/r_e
140
100
60
20
γ = 1.3
γ = 1.25
γ = 1.20
20
60
100
140
180
220
260
300
360
x/r_e

Figure 10

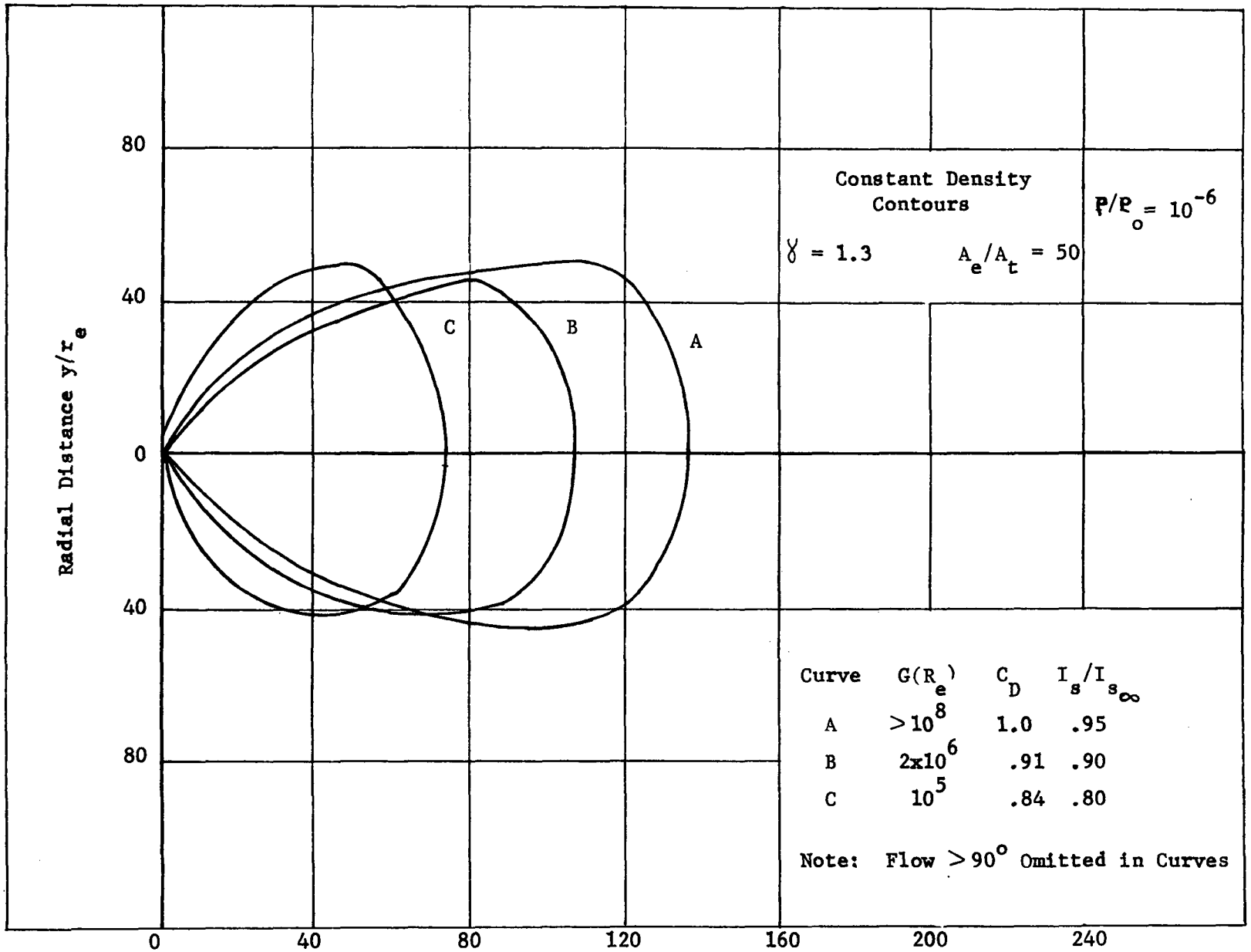
Constant Density Contours
$\gamma = 1.3$
$A_e/A_t = 50$
$P/P_o = 10^{-6}$
A
B
C
Curve $G(R_e)$ C_D I_s/I_{s_∞}
A $>10^8$ 1.0 .95
B $2x10^6$ .91 .90
C 10^5 .84 .80
Note: Flow $>90^o$ Omitted in Curves
Radial Distance y/r_e
Axial Distance x/r_e
80
40
0
40
80
0
40
80
120
160
200
240

Figure 11

jet during the nozzle expansion process and will exit with the jet. The subsequent trajectory of the particles is of importance when considering the possible interference of this effluent with other parts of the Space Station and the overall mission of the spacecraft.

The particulate material is carried in the jet through friction with the gaseous media. The gases expand and turn as described in the previous report on resistojet plume flow. Due to the inertia of the particles, they cannot follow the gaseous expansion exactly but will only follow the gas flow through the flow regime where the frictional drag is appreciable. As the gas flow expands and the density decreases, the jet drag reduces and the particles become essentially free bodies. This rarefaction is complete when the mean free path of the gas flow materially exceeds the particle diameter. In the continuum region of flow the drag acceleration of the particle is given by

$$\bar{a}_p = -\tfrac{9}{2} \frac{\mu}{\rho_p a^2} (\bar{u}_p - \bar{u}_g)$$

In the free molecular flow regime, the drag acceleration is given by

$$\bar{a}_p = \frac{2}{\sqrt{\pi}} \sqrt{2RT}\, \frac{\rho}{\rho_p a} (\bar{u}_p - \bar{u}_g)$$

The latter equation will only apply when the mean free path L greatly exceeds the radius a. This condition occurs for the resistojet application

$$L/a \cong \frac{\rho_0}{\rho}\, 10^{-9}/a \qquad \text{for methane}$$

with 3 atm chamber pressure and (a) measured in cm. For (a) equal 10^{-2} cm this condition occurs when ρ_0/ρ exceeds 10^7 in the plume. For the remainder of this analysis, the continuum regime of flow will be analyzed, and the drag outside of this regime will be neglected for simplicity.

To estimate the particle trajectory in the plume, the acceleration of the particles will be analyzed in the cartesian coordinate system, with origin at the nozzle centerline. The accelerations can be described as

$$a_{px} = u_{px} \frac{du_{px}}{dx} = -\tfrac{9}{2} \frac{\mu}{\rho_p a^2} (u_{px} - u_{gx}) \qquad a_{py} = u_{py} \frac{du_{py}}{dy} = -\tfrac{9}{2} \frac{\mu}{\rho_p a^2} (u_{py} - u_{gy})$$

The gas velocity at any point in the jet is a very complex function of the geometry. However, for approximation purposes there are simplifications that are possible. First, it is assumed that the particles entering the nozzle are initially all axial in flow direction at the exit gas velocity. The gas flow is assumed to take on the velocity and direction at the nozzle exit that it has in the far distant field. This assumption will result in slightly greater particle turning than is actually experienced and is conservative in its effect on the cone of particles. The gas velocity function under the assumptions is

$$u_{gx} = V_{MAX} \cos\theta \qquad u_{gy} = V_{MAX} \sin\theta$$

These functions are substituted into the above

$$u_{px} \frac{d u_{px}}{dx} = -\frac{9}{2} \frac{\mu}{\rho_p a^2} (u_{px} - V_{MAX} \cos\theta) \; ; \; u_{py} \frac{du_{py}}{dy} = -\frac{9}{2} \frac{\mu}{\rho_p a^2} (u_{py} - V \sin\theta)$$

These functions are difficult to solve in the exact form, but certain approxmations can be applied for the problem at hand. Using linearized approximations for these equations the resultant predicted angled for the trajectory of particles is given by;

$$\tan\varphi = \frac{u_{py}}{u_{px}} = \frac{\varepsilon \sin\theta \left[\sqrt{2/\varepsilon} - 1 \right]}{\frac{u_e}{V_{MAX}} \left[1 + \varepsilon \left(\cos\theta - \frac{u_e}{V_{MAX}} \right) \cos\theta \left(\frac{V_{MAX}}{u_e} \right)^2 \right.}$$

In this function

$$\varepsilon = 9/2 \, \mu r_0 / \rho_1 a^2 V_{MAX} \ll 1$$

where μ is the gas viscosity, r_0 is the radius from the nozzle apex to the outermost plume contour of continuum flow (about density ratio 10^{-7}), ρ_p is particle density, a the particle radius, and V_{MAX} as before.

2.2.5 Vapor condensation in the exhaust

The ability of vapor exhaust products to condense in the exhaust jet will depend upon the vapor pressure characteristics of the fluid relationship to the partial pressure of the vapor in the exhaust mixture. For the biowaste

resistotjet propellant of interest, water, carbon-dioxide and methane are the principal condensable species. The traces of oxygen and nitrogen are very small and are quite similar to the more prevalent methane in vapor pressure characteristic. Therefore, they may be assumed to follow the methane bahavior with small error. If the vapor pressure equals the partial pressure in the exhaust at a given exhaust temperature then condensation can occur. Whether condensation does occur in a flow situation depends upon the presence of suitable nucleation sites and sufficient time for molecular collisions. In general, some supersaturation can be expected in all cases of flow situations.

The Clausius-Clapyron relation of thermodynamics is used to approximate the vapor pressure-temperature characteristic of the fluid. This function is an exact one, except that in our approximation, the heat of fusion is assumed to be independent of temperature and the vapor phase is assumed to be a perfect gas when far from saturation. The result is the function

$$\frac{d \ln P}{d \ln T} = - \frac{\Delta H_{fg}}{RT}$$

which integrates to

$$\ln P = - \frac{\Delta H_{fg}}{RT} + \text{CONSTANT}$$

This function has been used to curve fit the vapor pressure for water, carbon-dioxide and methane. The results are:

$$\log_{10} P = \frac{-516}{T} + 4.77 \qquad \text{for methane}$$

$$\log_{10} P = \frac{-1365}{T} + 7.03 \qquad \text{for carbon-dioxide}$$

$$\log_{10} P = \frac{-2180}{T} + 5.78 \qquad \text{for water}$$

In these relations, P is in atmospheres and T in ^{o}K.

The prospect of condensation of a vapor in the exhaust occurs when the jet exhibits a flow static temperature below the above predicted saturation temperature at a given pressure. In this determination the partial pressure of the vapor must be accommodated since the vapor is only one constituent of the

mixture. The prediction of condensation is conservative, in that considerable supersaturation can be exhibited by the flow. The predictions of this analysis are to be used as indicators of potential condensation problems and detail treatment of the nucleation and growth of condensate, and the attendant supersaturation are outside the scope of this study. Calculations using the model predictions are presented in a subsequent section.

2.2.6 Condensation on adjacent components

The incident flux of biowaste exhaust upon adjacent spacecraft surfaces can cause accumulation of a condensate film under certain conditions. If the adjacent surface is cold, such that its capacity to reevaporate is low, the condensate will accumulate. The continuity of mass function for this phenomena is

Rate of change of surface film = condensation rate - evaporation rate.

The condensation rate may be related to the arrival rate of biowaste exhaust through the use of a condensation coefficient, i.e., the fraction of incident molecules that condense. This nature has been found to be approximately unity for the gases of interest. The evaporation rate of a perfect gas into vacuum is given by

$$\dot{N} = \frac{P_v}{\sqrt{2\pi m k T}}$$

where P_v is the vapor pressure, m the molecular mass, k is Boltzmann's constant and T the surface temperature. To determine the condition where the condensation rate just equals the evaporation rate, the incident flux is equated to the evaporative flux. At this condition the surface film will be at the incipient buildup condition. The incident flux is a function of the position of the target in the plume. The plume isodensity contours and related velocity predictions describes the incident flux on the target. Therefore, it is possible to define the minimum arrival rate Γ_{ao} that will cause incipient film

condensation. This limit is

$$\Gamma_{a0} = \frac{P_v}{\sqrt{2\pi k m T}}$$

The vapor pressure characteristic of the biowaste vapors was established in section 2.2 to be of the form

$$\ln_{10} P_v = -A/T + B$$

combining the above results in

$$\Gamma_{a0} = \frac{0.835 \times 10^{27}\ 10^{-A/T+B}}{\sqrt{M_v T}} \quad \text{molecules/cm}^2\text{sec}$$

where M_v is the vapor molecular weight in AMU.

The mass flux of exhaust impinging the target surface is given by

$$\dot{m}_{a0} = \chi_v \rho_0 (P/\rho)\, V/V_{MAX}\, V_{MAX} \sin\alpha$$

where χ is the mole fraction of vapor in the exhaust, and α is the angle between the target normal and the influx velocity vector. The impingement flux is a function of the plume shape and geometry. The evaporative flux is a function of the target temperature and the vapor pressure function of the vapor of interest.

For calculation purposes, the V_{MAX} function may be evaluated as

$$V_{MAX} = \sqrt{\frac{2\gamma}{\gamma-1} g_0 R T_0}$$

2.2.7 Exhaust lifetime in the vicinity

The lifetime of the exhaust in the vicinity of the spacecraft is important in estimating the residual effects of the jet between firings and between orbits. At the altitude of interest in this study, i.e., 200-300 nmi. (370-500 km), the residual atmosphere is still significant. The ambient density in this altitude range varies from 10^8 to 10^9 particles/cm^3 with 10^5 to 10^6 being the range of charged particle number density, the remainder being neutrals. The equivalent temperature of these particles is approximately 1500°K. For methane at 3 atm pressure and ambient temperature, the resistojet

chamber gas density is 10^{20} molecules/cm^3. To reduce to the ambient density, the gases must diffuse to a density of 10^{-11} to 10^{-12} of the chamber value. At plume density contours of 10^{-6}, as was plotted in the last monthly report, the plume dominates the environment. Using the plume theory developed, the jet density would decay to the ambient density of space at a distance from the nozzle given by

$$X = 0.5 \times 10^6 \, r_t$$

For a typical resistojet with r = 0.05 cm, this results in a distance of 2.5×10^4 cm, or about 830 ft. Therefore, along the jet axis, the plume dominates the environment for a distance approaching 300 m (1000 ft) if other interactions can be neglected. This distance is large with respect to the spacecraft dimension and if there are numerous jets, then there will be many such exhaust cones extending into space.

Some of the interacting forces involved are gravity, drag, and solar pressure. Consider the attractive force of gravity by the spacecraft in the particles and gases. To do this, it is helpful to compute the escape velocity from the spacecraft as a gravitational body. The escape velocity is

$$u_{escape} = \sqrt{G M_s / R_s}$$

For spacecraft mass of 140,000 kg and a radius of 10 meters, this escape velocity is 10^{-4}cm/sec. This is a very small velocity with respect to typical gas velocity and will not be significant as an effect on the gases in attracting them. Low velocity particulate debris may be affected however. The gravity attraction of the spacecraft is approximately 10^{-5} cm/sec^2 or about 10^{-8} g_o compared with earth's surface.

When considering the particulate material there are several life limiting features. If the material is condensate of a jet vapor, the particles

will re-evaporate through interaction with the ambient atmosphere. Sharma, et al, reporting in the December 1971 Journal of Spacecraft and Rockets have analyzed the life in space of water ice and found that the radius decays in time as

$$r_p = r_{op}\, e^{-t/\tau}$$

where τ is an evaporative time constant, which for water is about 1000 min. Thus, the particles decay in radius by a factor of 1/e every 1000 min. Therefore, the particle lifetime is long compared to an orbital period. Sharma reports that the τ for oxygen ice is about 100 minutes.

In addition to the gravity pressure, the particles will be acted in by the solar flux. This will generate a solar light pressure on the particles and deflect their trajectories. The solar radiation pressure is given by

$$P_R = 5 \times 10^{-6} \text{ kg m}^{-1} \text{ sec}^{-2}$$

For a particle of radius a and density

$$\text{acceleration} = P_R \pi a^2 / 4/3 \pi a^3 \rho = 3/4\, P_R / a\rho$$

For small particles of size a = 25μm and density ρ = 1 g/cc this acceleration is

$$\text{acceleration} = .15 \times 10^{-3} \text{ m/sec}^2 = 1.6 \times 10^{-4} g_o$$

At this acceleration level, the range that a slow particle will achieve is $\frac{1}{2}at^2$ in a specified time. In an orbital period of 90 min (5400 sec.) this range change is approximately 4 km and the particle will be outside the region of the next orbital pass. The solar pressure acceleration of $1.5 \times 10^{-4} g_o$ is much larger than the gravitational attraction of $10^{-8}\ g_o$ and therefore dominates gravity attraction.

Particulate material from the jets will be acted upon by the solar light pressure during the illuminated portion of the orbit and accelerate away from the spacecraft. One question which arises is, will the jet effluent remain in the proximity long enough that subsequent orbits of the spacecraft will pass through the debris. The gaseous material and high velocity particulate material will have a large relative velocity with respect to the space station and will dissipate rapidly even without the solar influence. For example, the jet velocity will approach the maximum speed of

$$V_{MAX} = \sqrt{\frac{2\gamma}{\gamma-1} gRT_o}$$

which is for methane at 27°C equal to 3400 fps or 1000m/sec. relative to the spacecraft. Therefore, the gaseous material will not remain or persist as a problem to the space station.

2.3 Model Applications

Having completed the analyses required to develop the predictive models described in the preceding section, representative calculations were performed to assess the conditions presented by typical biowaste propellant compositions and thermodynamic states.

2.3.1 Biowaste resistojet plume flows

The biowaste propellant mixtures and temperatures of interest exhibit specific heat ratios in the range 1.2 to 1.3. as presented in Table 1. Using the parameters of the thrusters of interest, the value of the G(Re) function is typically 10^6. This yields a $C_D = 0.89$ and $I_s/I_{s\infty} = .885$ from Figure 8. Referring to Figure 9, this gives a value of $(\gamma-n) = 0.6$ for the flows of interest. For the three γ values exhibited in the flow situations of interest ($\gamma = 1.2$@1000°K except for water, $\gamma = 1.3$ at 300°K for all and $\gamma = 1.25$ @ 500°K for all except water) the corresponding n values are as follows:

γ	n
1.20	1.14
1.25	1.19
1.30	1.24

Reference to Table 1 indicates that these three values of γ span the range of interest from 300°K to greater than 1000°K. To compute the plume shapes and properties it was necessary to determine the V/V_{max} velocity ratios. For the above cases, these velocity ratios are presented in Table 3, calculated from the analytical model developed.

Table 3

Velocity Ratio

γ	ρ_o/ρ	V/V_{max}
1.3	10^4	.956
1.3	10^5	.978
1.3	10^6	.988
1.3	10^7	.995
1.25	10^4	.930
1.25	10^5	.960
1.25	10^6	.978
1.25	10^7	.987
1.20	10^4	.885
1.20	10^5	.936
1.20	10^6	.957
1.20	10^7	.973

Typical plume density contours were presented in section 2.2 in Figures 7 through 9 . For convenience in representation of the data, the coordinates have been non-dimensionalized by the nozzle exit radius r_e.

The conclusion to be drawn from these results are as follows

1. The viscous jet plumes spread appreciably greater than the predicted inviscid jet does. This will give appreciably greater flows off the jet axis, and particularly at high angles off axis where the inviscid solution predicts negligible flow.
2. The decay of density on the axis of the jet is more rapid for the viscous jet than for the inviscid jet.
3. Resistojet operation at high temperature ($> 1000^{\circ}K$, low thrust (.12N) and low pressure (1 atm) puts the flow well into the viscous effects regime and accentuates the spreading phenomena described in 1. and 2. above. High temperature and low thrust may have to be avoided in some locations on the spacecraft jets to preclude side and back-flow effects.

2.3.2 Condensation of the exhaust

The conditions under which the biowaste propellant mixtures could condense were defined in section 2.2.5 . In this application section, the properties of the propellants are inserted in the model to describe the prospects of condensation under the various operating conditions. Condensation can occur either in the nozzle flow or in the plume flow. Condensation in the nozzle flow is potentially the more serious since nozzle blockage could occur. Also, the earlier in the flow that condensation occurs, the larger and more numerous the particles generated will be since there will be a corresponding larger residence time at higher density conditions for droplet growth. The principle condensibles are water, carbon dioxide and methane, in that order.

2.3.2.1 Condensation of the molecular sieve

For the molecular sieve (carbon dioxide) output described as mixture A in Table 2 the condensation prospects were evaluated. This required the evaluation of the viscous parameter G (Re) for the flow conditions of interest. These conditions were

Temperature (^{o}K)	300, 500, 1000, 1600
Thrust (N)	.12, .48
Pressure (atm)	1, 3

The viscous parameter varied from $.2 \times 10^{7}$ to 2×10^{4} for these cases. The results of the calculations are described below.

For the molecular sieve biowaste propellant source, the following conclusions may be made regarding condensation in the plume and nozzle flow.

a) The effect of pressure from 1 to 3 atm is not significant. This is equivalent to a change in temperature of about 30^{o}K and therefore has little influence on the flow. In general, the higher the pressure, the more likely is the condensation in the nozzle or plume.

b) The flow will show condensation, or incipient condensation, in the nozzle at chamber temperature up to 500^{o}K. At 300^{o}K it is very likely and at 500^{o}K it depends upon pressure. At 3 atm and 500^{o}K it is likely to condense. At 1 atm and 500^{o}K it is not. Thrust level has a small influence in the range from 25 mlb to 100 mlb on nozzle condensation.

c) Condensation in the continuum flow portion of the plume is not likely for temperatures above 1000^{o}K and with the thrust levels and pressures of interest.

d) Between 500°K and 1000°K chamber temperature the vapors are likely to condense in the near plume but outside the nozzle proper.

e) The thrust does not greatly influence the results. At lower thrust the condensation limits on chamber temperature would reduce slighly because of the viscous effects in the nozzle on the thermodynamics.

2.3.2.2 Sabatier output

In the Sabatier output stream, methane, water and/or carbon dioxide could condense. This output is described as mixture B in Table 2. Temperatures to 1000°K were evaluated. At temperatures above this, the methane can be expected to undergo potentially troublesome dissociation. All three major constituents were investigated for condensation. The results of these analyses are:

1. Condensation of methane is not predicted at any of the conditions of flow studied and, therefore, does not represent a condensation problem.
2. The residual water vapor in the flow will be capable of condensation in the nozzle at temperatures below approximately 1000°K. However, the quantity of water is relatively small (1.5%) and should not represent a problem of flow blockage.
3. Condensation of the carbon dioxide in the nozzle flow is marginal at 300°K chamber temperature and not possible at higher temperatures. The carbon dioxide will condense in the plume at 500°K and above, but is not an appreciable weight fraction of the flow (5.9%).

The viscous parameter for the Sabatier output varied from 3×10^6 to

8×10^8 for the flow condition of interest. This flow is more viscous than the sieve output, and if it were operated at temperatures above $1000^{\circ}K$, the viscous pluming would be significantly worse than that of the inviscid prediction.

2.3.2.3 Water supplement

The use of water as a supplemental propellant is of interest for certain mission periods. It was correctly anticipated that water is potentially the greatest problem regarding condensation. The viscous parameter for water flow varied from 2×10^8 to 10^6. This indicates that water flows are also significantly affected by viscous effects. Temperatures of $500^{\circ}K$ and above were studied, because below this the water is in a liquid state at the pressures of interest (vapor pressure 3 atm at $400^{\circ}K$). The conclusions to be drawn are:

1. All cases at $500^{\circ}K$ will show condensate in the nozzle.
2. At $1000^{\circ}K$, only the 1 atm, 25 mlb nozzle flow will be free of condensate; all others will be at various degrees of condensation conditions.
3. Above about $1100^{\circ}K$ all of the flows will be outside the condensation envelope for the nozzle.
4. Condensation in the plume is predicted for all temperatures below $2200^{\circ}K$ in the chamber.

2.3.3 Particle trajectories computation

The trajectory of particles in the jet is significant from a contamination standpoint. Any particles in the vicinity of the spacecraft can scatter optical signals and impinge surfaces at relatively high velocities (km/sec) and generate damage. The analysis of particle trajectories was treated in section 2.2.4. The predictions have been prepared for the biowaste

gas mixtures of interest and the pressures, temperatures, etc. that are appropriate to the biowaste resistojet application.

The particle deflection formula was found to be

$$\tan\varphi = \sqrt{2\varepsilon}\,\sin\theta$$

where φ is the cone ½ angle of the particle and θ is the angle from the jet axis that the gas flow takes. The parameter r_o described in section 2.2.4 varies with the plume shape for each thrust, pressure, gas, etc. For most plumes of interest, it was found that the parameter $\sqrt{r_o}\sin\theta$ maximized, i.e., gave the largest particle deflection angle at $\theta = 30^\circ$ and r_o typically 250 nozzle exit radii. This yields an approximation for $\sqrt{r_o}\sin\theta$ of about $8\sqrt{r_e}$. The defining relation for $\tan\varphi$ then becomes, approximately the following

$$\tan\varphi = 24\sqrt{\frac{\mu r_e}{\rho_p a^2 \sqrt{\frac{2\gamma}{\gamma-1}RT_o}}}$$

For any gas the viscosity μ varies in temperature but independent of pressure. This variation is, by kinetic theory, proportional to $\sqrt{T}$. In actuality, it often varies by T^n where n is from 0.5 to 0.8 with 0.6 a common number. As a result, it can be seen that the particle trajectories will be essentially independent of chamber temperature for a given gas selection and only one temperature need be evaluated for a specific biowaste mixture, except for minor variations that take place in γ versus temperature. The particle density (ρ_r) can be assumed to be near s.g. of 1 for the contaminants of interest, and the particulates may vary from 1-100 μm in size. The nozzle exit radius is proportional to the throat radius. The throat radius of a resistojet is a function of thrust level and the gas of interest. For the biowaste gases of interest, the throat radius is given approximately by

$$r_t = \sqrt{F/P_o}$$

which for $F = 25$ mlb (.11N)

$P_o = 1$ atm (10^5 N/M^2)

$r_t \approx 10^{-3}$m

Also, from the above discussion

$$\rho = 10^3 \text{Kg/m}^3$$

$$a = 10^{-6}\text{m to } 10^{-4}\text{m}$$

Evaluating at 300°K for the gas properties required results in the following table for values of viscosity and V_{MAX} for the various biowastes.

Gas Flow Properties for Particulate

Trajectory Calculations @ 300°K

Mixture	Source	μ (Nm/sec)	V_{MAX} (m/sec)
A	Mole sieve	2×10^{-5}	730
B	Sabatier	2×10^{-5}	1210
D	Water	1.2×10^{-5}	1140

Typical values of the parameter $\sqrt{2\epsilon}$ were computed for the biowaste mixtures of interest, and from this the turning angle of particulates can be computed.

The results of the applications analysis regarding the particulates are summarized below.

A. For a given biowaste, the particle cone will be essentially independent of chamber temperature. The only effect of chamber temperature will be a small variation of γ in the plume, and a very small effect on gas viscosity as discussed. The plume shape changes somewhat, but not sufficiently to alter the magnitude of the particle turning.

B. The 100 μm particles are contained with 5° of the nozzle axis for all the biowaste gases, pressures, thrusts, etc. studied. Therefore, the particles of large size will be well collimated along the axis. The small (10 μm) particles can be spread further, out to about 30^{0} from the axis. Very small (1 μm) particles can be expected to have an even larger conical angle. However,

TABLE 4

Particulate Turning Angle for Typical Biowaste Mixtures and Particle Sizes

Mixture	Thrust (mlb)	Pressure (atm)	Particle Size (μm)	Particle Turning Angle (^{o})
A	25	1	100	2.3
A	25	3	100	1.8
A	100	1	100	3.2
A	100	3	100	2.5
A	25	1	10	21.8
A	25	3	10	17.1
A	100	1	10	29.2
A	100	3	10	23.7
B	25	1	100	2.9
B	25	3	100	2.1
B	100	1	100	4.2
B	100	3	100	3.1
B	25	1	10	27.1
B	25	3	10	23.1
B	100	1	10	34.5
B	100	3	10	29.2
D	25	1	100	2.0
D	25	3	100	1.5
D	100	1	100	3.0
D	100	3	100	2.2

particles this small do not represent a large source of damage potential.

C. At a given thrust, the higher pressure cases show less turning of the particulates. This is due to the smaller nozzle and plume dimensions of these jets and, therefore, the shorter residence time in the plume.

D. Higher thrust causes larger turning angles for the same reason as in C above.

E. The various physical properties of the biowaste gases, namely viscosity, V_{MAX}, γ are such that in any application there is very little difference in particle turning result from one to the other of the biowaste.

F. For the range of parameters studied, the particle cone is much less in apex angle than the plume proper and simple line-of-sight precautions may be taken. Only the smallest particles, less than 10μm, in radius need be considered as turning appreciably.

The above analyses and prediction could be used to determine plume opacity calculations once the particle number density is determined or estimated. The plume opacity, or scattering analysis is outside the scope of the current study. The particle turning calculations made for the biowaste resistojet appear to be the first publication of this concern for small jets. Although the primary flows of the biowaste gases will be filtered to remove particulates, any particulates added downstream of the filter due to condensate, salt precipitation, or material flaking will be carried off in the exhaust. In a prior effort under this contract, the amount of salts present in the water were estimated to be of the order of several hundred grams per thruster over the life of the thruster. This assumed that there was no separate vaporizer to trap deposited salts.

3.0 TESTING AND FLIGHT EXPERIMENTS

It is recommended that ground simulation tests be conducted at the thruster level using representative biowaste mixtures. The key simulation required is that of the water content in the biowaste. To be meaningful, the tests should be conducted in a facility of sufficient size and pumping ability to achieve a full continuum flow plume. This can be accomplished in chambers of a size of a few meters characteristic length. The key data to be obtained is the verification of the off-axis flow predictions for condensation on targets placed in the low density portions of the stream.

Flight experiments using resistojets with simulated biowaste would be of value to determine effects on candidate or actual experiments. The emphasis should be placed on two experimental areas a) those with cold sensors where condensate would tend to accumulate and b) imaging or viewing experiments in the wavelength range where particulate light scattering and absorbtion would be critical. Biowaste resistojet operating parameters would be selected so that the temperatures and flows would span the predicted range of incipient problems described in earlier sections of the report. The specific experiment that would verify the contamination aspect of biowaste resistojets is one using water laden carbon dioxide as propellant. Operation at a range of temperatures from ambient to about 1600^{o}K could be accomplished in sequential steps, with non-thrusting periods between to obtain reference states for experimental observations.

3.1 Ground Test Recommendations

Ground simulation tests to verify the predicted biowaste contamination effects are essential to the continuation of the biowaste resistojet development program. Considerable test data should be accrued before committing to a flight test verification of contamination or a flight payload design. Two features of the potential contamination problem were identified in the study and stated above, namely plume shape for small jets, and condensation effects.

The ground tests could be conducted with humidified carbon-dioxide propellant since both water and CO_2 are the most condensible candidate compounds. Dew-point of the CO_2 of $5^{o}C$ should be used as being representative of the spacecraft condenser heat sink. If another cold source is available, then the dew point appropriate to the available source should be used. Additional tests should be conducted with water alone, if this source continues to be an interesting make-up propellant for high-impulse demand periods. The tests should measure, through beam scattering techniques, the opacity of the jet plume under various thruster temperatures in the range of 300 - $1600^{o}K$. Also, the region of condensation upon adjacent surfaces should be investigated through the use of chilled blocks arrayed around the plume area at temperatures representative of the spacecraft sensors. The use of quartz crystal micro-balances as indicators is an alternative, but the response of these would require integration since it would be difficult to determine whether the deposited material was condensate or adsorbed chemicals. Testing should be conducted in a chamber providing ambient densities approximately 10^{-6} or less of the thruster chamber density.

3.2 Flight Test Experiment

The flight test experiment to verify predicted biowaste propellant exhaust contamination could best be performed as an auxiliary test on an experimental payload using actual flight sensors and optics. After completion

of the primary mission, the resistojets could be operated at conditions indicated by the results of the ground test to be conducive to contamination conditions. The same carbon-dioxide and/or water propellants should be used in these tests. Capability to test with humidified carbon-dioxide and water separately would be very desirable. If the water proves to be a continuing potential problem, it use as a propellant supplement would have to be re-evaluated.

4.0 CONCLUSIONS AND RECOMMENDATIONS

The analytical studies performed have resulted in the preparation of a number of interesting conclusions. These conclusions must be considered to be unsubstantiated until the verification testing suggested has been completed. The pertinent conclusions of the study performed are:

Plume shape

The resistojet thrusters in the .12 - .50N (25 - 100 mlb) range will exhibit plumes of greater apex angle for a given density contour than would a scaled inviscid jet. Appreciable flows at 30-45^{o} off-axis can be expected. The flow occurring at angles greater than 90^{o} can be expected to be substantially greater than for an inviscid solution prediction.

Operation at low thrust, low pressure and high temperature accentuate this pluming due to increased viscous effects in the nozzle flow. Operation at 500^{o}K, 3 atm and .25N or greater will cause the flow to be less viscous dominated and more like an inviscid jet.

4.1 Condensation Effects

Water will prove to be a condensible exhaust constituent for all biowaste sources unless low dew points and/or high chamber temperatures are used. At the expected water content of the Sabatier effluent, the chamber temperature should be held above 1000^{o}K to preclude condensation in the nozzle flow. The use of pure water should be limited to high temperature operations to preclude condensation effects. This is consistent with the intent of the use of water as a supplement. When a supplement is required, it should be used at its greatest impulse effectiveness, i.e., high temperature. The recommendation to use high temperatures to preclude condensation effects is countered by the desire to use low temperatures to minimize viscous pluming. The net result is that the thrust level may have to be elevated and operations

conducted at intermediate (500 - 1000°K) temperatures to achieve a compromise between the two effects.

Condensation on cold targets is possible with any of the biowastes depending upon the specific location with respect to the jet (the surface temperature and the biowaste resistojet) operating temperature and pressure. A detail analysis of each case is required to provide any conclusions. Given jet conditions, isotherms could be plotted in the jet plume on which targets at the specified temperature would condense out biowastes (water, carbon dioxide).

4.2 Particle Trajectories

The analysis predicts that the particle turning angle is essentially independent of operating temperature and dictated largely by particle size. Each particle size will be restricted to a conical plume which increases in angle as particle size is reduced. The angles of particle turning are much less than the plume envelope and so should not present a problem if the plume gas impingement does not.

4.3 Effluent Life In The Vicinity

The biowaste resistojet effluent is traveling at high velocity (km/sec) and is largely directed in the plume away from the craft. Both of these features make the dumping of biowaste vapors through the resistojet nozzles superior to simple ambient venting when considering possible residual effects, i.e., contamination. Even the viscous related flow effects which cause the resistojet flow to expand off-axis would not create the severity of back-flow that can be expected from simple venting. Also, the simple vent will probably require modest heating to preclude "icing" and subsequent flow stoppage. Therefore, even the relatively simple ambient vent takes on complicating features. The vent heating would require sequencing and power control to conserve energy on the craft. The biowaste vapors when expanded in the resistojet at modest temperatures (500°K) are mobile and directed within relatively tight bounds of

prediction. The same cannot be said of simple vents.

Several papers presented at the AIAA 9th Electric Propulsion Conference of April 17-19, 1972 were of considerable value in preparing the recommendation of this report. Notable of these was the work reported by J. M. Kallis, et al, entitled "Viscous Effects on Biowaste Resistojet Nozzle Performance." In this work, the nozzle specific impulse and associated flow characteristics of biowaste propellants were presented. This data was useful in the verification of the assumed simplified model of viscous flow developed in the current work.

5.0 BIBLIOGRAPHY

1. Baurer, T. et al.: "External Spacecraft Contamination Modeling and Countermeasures." General Electric Co., Philadelphia, Pa., June 1970.

2. Blair, P.M.; and Levin, Herman: "Study of the Combined Effects of Space Environmental Parameters on Space Vehicle Materials." Quarterly Progress Report No. 4, NASA, Marshall Space Flight Center, Huntsville, Alabama, Nov. 30, 1968.

3. Day. B. P.; and Fearn, D. G.: "A Review of Electric Propulsion Research in the United Kingdom." AIAA Paper No. 69-299, AIAA 7th Electric Propulsion Conference, Williamsburg, Virginia, March 3-5, 1969.

4. Frazine, D. F.; and Cox, G. S.: "Instrumentation for Evaluating Effects of Plume Contamination on Optical Properties of Spacecraft Surfaces." Aro, Inc., May 1970.

5. Gibson, Robert N., Jr.; and Cygnarowicz, Thomas A.: "Design and Performance of a Thermal Storage Resistojet." AIAA Paper No. 67-662, AIAA Electric Propulsion and Plasmadynamics Conference, Colorado Springs, Coloroado, September 11-13, 1967.

6. Goldin, D. S., et al.: "Integration of Science Payloads with Multimission Electrically Propelled Spacecraft." AIAA Paper No. 70-1141, AIAA 8th Electric Propulsion Conference, Stanford, Calif., August 31-September 2, 1970.

7. Halbach, Carl R.; and Yoshida, Ronald Y.: "Development of a Biowaste Resistojet." AIAA Paper No. 70-1133, AIAA 8th Electric Propulsion Conference, Stanford, California, August 31-September 2, 1970.

8. Hall, David F.: "Evaluation of Electric Propulsion Beam Divergence and Effects on Spacecraft." NASA, September 2, 1969.

9. Hallgren, D. S.; and Hemenway, C. L.: "Direct Observation of Particulate and Impact Contamination of 'Optical' Surfaces in Space." COSPAR, Plenary Meeting, 11th, Tokyo, Japan, May 9-21, 1968.

10. Haukohl, J.; and Spradley, L. W.: "Multi-Specie Condensation in Expanding Flows." Lockheed Missiles and Space Company, Huntsville, Alabama, June 1970.

11. Jackson, F. A., et al.: "An Operational Electrothermal Propulsion System for Spacecraft Reaction Control." AIAA Paper No. 66-213, AIAA Fifth Electric Propulsion Conference, San Diego, Calif., March 7-9. 1966.

12. Kytola, J. W.; and Danta, R. C.: "Contamination Sources Considered for the VELA Spacecraft Mission." Vela Satellite Program, September 1965.

13. Llinas, J.: "An Investigation of Rocket Plume Impingement Effects on the Manned Orbital Workshop." Cornell Aeronautical Lab., Inc., Buffalo, N. Y., Dec. 1969.

14. Martinkovic, P. J.: "Monopropellant Exhaust Contamination Investigation." Air Force Systems Command, Edwards AFB, Calif., Nov. 1967 - Dec. 1968.

15. Murch, C. K.; and Krieve, W. F.: "Electrothermal Thruster Performance with Biowaste Propellants." AIAA Paper No. 70-1161, AIAA 8th Electric Propulsion Conference, Stanford, Calif., August 31-September 2, 1970.

16. Page, Russell, J.; and Short, Robert A.: "Ten-Millipound Resistojet Performance." AIAA Paper No. 67-664, AIAA Electric Propulsion and Plasmadynamics Conference, Colorado Springs, Colorado, September 11-13, 1967.

17. Pisciotta, A., Jr.; and Eusanio, E.: "Subsystem Analyses for a MORL Resistojet Control System." AIAA Paper No. 67-721, AIAA Electric Propulsion and Plasmadynamics Conference, Colorado Springs, Colorado, September 11-13, 1967.

18. Pugmire, T. Kent; and Shaw, Robert: "Applied Resistojet Technology." AIAA Paper No. 70-211, AIAA 8th Aerospace Sciences Meeting, New York, N. Y., January 19-21, 1970.

19. Pugmire, T. K., et al.: "Thermal and Material Considerations Pertinent to the Biowaste Resistojet." AIAA Paper No. 70-1135, AIAA 8th Electric Propulsion Conference, Stanford, Calif., August 31-September 2, 1970.

20. Pugmire, T. K.; and Lund, Williams: "ATS-III Resistojet Thruster System Performance." AIAA Paper no. 68-553, AIAA 4th Propulsion Joint Specialist Conference, Cleveland, Ohio, June 10-14, 1968.

21. Shapiro, H.; and Hanyok, J.: "Monomolecular Contamination of Optical Surfaces." NASA, Goddard Space Flight Center, Greenbelt, Md., June 1968.

22. Shaw, R., et al.: "Ammonia Resistojet Station Keeping Subsystem Aboard Applications Technology Satellite (ATS)-IV." AIAA Paper No. 69-296, AIAA 7th Electric Propulsion Conference, Williamsburg, Virginia, March 3-5, 1969.

23. Sodek, B. A.: "A TM Optical Contamination Study: Reaction Control System Rocket Engine Space Plume Flow Fields." Brown Engineering Co., Inc. Huntsville, Alabama, April 1968.

24. Tobias, Ivan I.; and Kosson, Robert L.: "A Resistojet System for Attitude Control of Unmanned Earth Satellites." AIAA Paper No. 66-225, AIAA Fifth Electric Propulsion Conference, San Diego, Calif., March 7-9, 1966.

25. White, Arthur F.: "Electrothermal Microthrust Systems." AIAA Paper No. 67-423, AIAA 3rd Propulsion Joint Specialist Conference, Washington, D.C., July 17-21, 1967.

26. Williams, T. N.: "Oil-Vapor Contamination of Satellite Optical Surfaces." Corrigendum to Technical Report 69055, Royal Aircraft Establishment, March 1969.